Technische Universität Chemnitz

Sonderforschungsbereich 393

Numerische Simulation auf massiv parallelen Rechnern

H. Harbrecht R. Schneider

Wavelet Galerkin Schemes for 3D-BEM

Preprint SFB393/02-05

Preprint-Reihe des Chemnitzer SFB 393

SFB393/02-05 **February 2002**

Contents

1 Wavelets on manifolds **2**

1.1 Wavelets and multiresolution analysis 2

1.2 Biorthogonal spline multiresolution on the interval 4

1.3 Wavelets on the unit square 8

1.3.1 Biorthogonal scaling functions 8

1.3.2 Tensor product wavelets 9

1.3.3 Simplified tensor product wavelets 9

1.3.4 Wavelets optimized with respect to their supports 12

1.4 Wavelets on domains and manifolds 12

1.4.1 Parametric representations of manifolds 13

1.4.2 Patchwise smooth wavelet bases 14

1.4.3 Globally continuous piecewise linear wavelets 16

2 The wavelet Galerkin scheme **23**

2.1 Discretization 23

2.2 A-priori compression 24

2.3 Setting up the compression pattern 26

2.4 Assembly of the compressed matrix 26

2.5 A-posteriori compression 28

2.6 Wavelet preconditioning 29

3 Numerical Results **30**

3.1 Dirichlet Problem 31

3.2 Neumann Problem 33

Author's addresses:

H. Harbrecht, and R. Schneider
TU Chemnitz
Fakultät für Mathematik
D-09107 Chemnitz

`http://www.tu-chemnitz.de/sfb393/`

Abstract

This paper is intended to present wavelet Galerkin schemes for the boundary element method. Wavelet Galerkin schemes employ appropriate wavelet bases for the discretization of boundary integral operators. This yields quasi-sparse system matrices which can be compressed to $\mathcal{O}(N_J)$ relevant matrix entries without compromising the accuracy of the underlying Galerkin scheme. Herein, $\mathcal{O}(N_J)$ denotes the number of unknowns. The assembly of the compressed system matrix can be performed in $\mathcal{O}(N_J)$ operations. Therefore, we arrive at an algorithm which solves boundary integral equations within optimal complexity. By numerical experiments we provide results which corroborate the theory.

Introduction

Various problems in science and engineering can be formulated as boundary integral equations. In general, boundary integral equations are solved numerically by the boundary element method (BEM). For example, BEM is a favourable approach for the treatment of exterior boundary value problems. Nevertheless, traditional discretizations of integral equations suffer from a major disadvantage. The associated system matrices are densely populated. Therefore, the complexity for solving such equations is at least $\mathcal{O}(N_J^2)$, where N_J denotes the number of equations. This fact restricts the maximal size of the linear equations seriously.

Modern methods for the fast solution of BEM reduce the complexity to a suboptimal rate, i.e., $\mathcal{O}(N_J \log^\alpha N_J)$, or even an optimal rate, i.e., $\mathcal{O}(N_J)$. Prominent examples for such methods are the *fast multipole method* [17], the *panel clustering* [20] or *hierarchical matrices* [19, 32]. As introduced by [1] and improved in [9, 10, 11, 12, 30], wavelet bases offer a further tool for the fast solution of integral equations. In fact, a Galerkin discretization with wavelet bases results in quasi-sparse matrices, i.e., the most matrix entries are negligible and can be treated as zero. Discarding these nonrelevant matrix entries is called matrix compression. It has been shown in [30] that only $\mathcal{O}(N_J)$ significant matrix entries remain.

Concerning boundary integral equations, a strong effort has been spent on the construction of appropriate wavelet bases on surfaces [7, 14, 15, 21, 26, 30]. In order to achieve the optimal complexity of the wavelet Galerkin scheme, wavelet bases are required with a sufficiently large number of vanishing moments. Our realization is based on biorthogonal spline wavelets derived from the multiresolution developed in [4]. These wavelets are advantageous since the regularity of the duals is known [33]. Moreover, the duals are compactly supported which preserves the linear complexity of the fast wavelet transform also for its inverse. This is an important task for the coupling of FEM and BEM, cf. [22, 23]. Additionally, in view of the discretization of operators of positive order, for instance, the hypersingular operator, globally continuous wavelets are available [2, 5, 14, 21].

The efficient computation of the relevant matrix coefficients turned out to be an important task for the successful application of the wavelet Galerkin method [13, 21, 27, 28, 30]. We present a fully discrete Galerkin scheme based on numerical quadrature. Supposing that the given manifold is piecewise analytic we can use a *hp*-quadrature scheme [21, 30] in combination with exponentially convergent quadrature rules. This yields an algorithm with asymptotically linear complexity without compromising the accuracy of the Galerkin scheme.

The outline of the present paper is as follows. In section 1 we the construction of suitable wavelet bases on manifold. We treat the also globally continuous wavelet bases which are required for the discretization of boundary integral operators of positive order. With these bases at hand we are able to introduce the fully discrete wavelet Galerkin scheme in section 2. We survey on several practical aspects like setting up the compression pattern, assembling the system matrix and preconditioning. In section 3 we present numerical results which confirm the theoretical results quite well. The accuracy of the Galerkin scheme has never been deteriorated by the matrix compression.

1 Wavelets on manifolds

For the treatment of boundary integral equations, wavelet bases defined on manifolds are required which provide besides an approximation power also a certain number of vanishing moments. This by itself is a nontrivial task. We apply the idea of [14, 21]. For sake of brevity we recall only some basics of this construction. Moreover, we focus mainly on piecewise constant and linear functions. The outline is as follows. First, we introduce the general concept of a biorthogonal multiresolution analysis. Then, we define wavelets on the interval $[0,1]$ which are brought to the unit square by tensor product techniques. Utilizing a domain decomposition strategy, these wavelets are lifted onto the manifold via parametrization.

1.1 Wavelets and multiresolution analysis

Multiresolution is by now a well-studied topic in signal processing. There are many excellent accounts about it, we refer the reader to the survey paper [6] and the references therein. Here we collect only some facts which are useful for our purpose. Let Ω be a domain $\in \mathbb{R}^n$ or manifold $\in \mathbb{R}^{n+1}$. Then, in general, a multiresolution analysis consists of a nested family of finite dimensional subspaces

$$V_{j_0} \subset V_{j_0+1} \subset \cdots \subset V_j \subset V_{j+1} \cdots \subset \cdots \subset L^2(\Omega), \tag{1}$$

such that $\dim V_j \sim 2^{nj}$ and

$$\overline{\bigcup_{j \geq j_0} V_j} = L^2(\Omega). \tag{2}$$

Each space V_j is defined by a single scale basis $\Phi_j = \{\phi_{j,k} : k \in \Delta_j\}$, i.e., $V_j = \operatorname{span}\{\Phi_j\}$, where Δ_j denotes a suitable index set with cardinality $|\Delta_j| \sim 2^{nj}$. A final requirement is that these bases are uniformly stable, i.e., for any vector $\mathbf{c} \in l^2(\Delta_j)$ holds

$$\|\mathbf{c}\|_{l^2(\Delta_j)} \sim \|\Phi_j \mathbf{c}\|_{L^2(\Omega)} \tag{3}$$

uniformly in j. Furthermore, the single scale bases satisfy a locality condition

$$\operatorname{diam}\operatorname{supp} \phi_{j,k} \sim 2^{-j}.$$

Instead of using only a single scale j the idea of wavelet concepts is to keep track to increment of information between two adjacent scales j and $j+1$. Since $V_j \subset V_{j+1}$ one decomposes $V_{j+1} = V_j \oplus W_j$ with some complementary space W_j, $W_j \cap V_j = \{0\}$, not necessarily orthogonal to V_j. Of practical interest are the bases of the complementary spaces W_j in V_{j+1}

$$\Psi_j = \{\psi_{j,k} : k \in \nabla_j = \Delta_{j+1} \setminus \Delta_j\}.$$

It is supposed that the collections $\Phi_j \cup \Psi_j$ are also uniformly stable bases of V_{j+1}. If

$$\Psi = \bigcup_{j=j_0-1}^{\infty} \Psi_j,$$

where $\Psi_{j_0-1} := \Phi_{j_0}$, is a Riesz-basis of $L_2(\Omega)$ we will call it a wavelet basis. We assume that these basis functions $\psi_{j,k}$ are local with respect to the corresponding scale j, i.e.,

$$\operatorname{diam}\operatorname{supp} \psi_{j,k} \sim 2^{-j}$$

and we will normalize them such $\|\psi_{j,k}\|_{L_2(\Omega)} \sim 1$.

We note that at first glance it would be very convenient to deal with a single orthonormal system of wavelets. But it was shown in [12, 30] that orthogonal wavelets are not completely appropriate for the efficient solution of boundary integral equations. For that reason we use biorthogonal wavelet bases. Then, we have also a biorthogonal, or dual, multiresolution analysis, i.e., dual single-scale bases $\widetilde{\Phi}_j = \{\widetilde{\phi}_{j,k} : k \in \Delta_j\}$ and wavelets $\widetilde{\Psi}_j = \{\widetilde{\psi}_{j,k} : k \in \Delta_j\}$ which are coupled to the primal ones via

$$(\Phi_j, \widetilde{\Phi}_j)_{L^2(\Omega)} = \mathbf{I}, \quad (\Psi_j, \widetilde{\Psi}_j)_{L^2(\Omega)} = \mathbf{I}.$$

The associated spaces $\widetilde{V}_j := \operatorname{span}\{\widetilde{\Phi}_j\}$ and $\widetilde{W}_j := \operatorname{span}\{\widetilde{\Psi}_j\}$ satisfy

$$V_j \perp \widetilde{W}_j, \quad \widetilde{V}_j \perp W_j. \tag{4}$$

Denoting likewise to the primal side

$$\widetilde{\Psi} = \bigcup_{j=j_0-1}^{\infty} \widetilde{\Psi}_j, \quad \widetilde{\Psi}_{j_0-1} := \widetilde{\Phi}_{j_0},$$

then, every $v \in L^2(\Omega)$ has a representation

$$v = \sum_{j\geq j_0-1}^{\infty} \sum_{k\in\nabla_j} (v, \psi_{j,k})_{L^2(\Omega)} \widetilde{\psi}_{j,k} = \sum_{j\geq j_0-1}^{\infty} \sum_{k\in\nabla_j} (v, \widetilde{\psi}_{j,k})_{L^2(\Omega)} \psi_{j,k}$$

and moreover

$$\|v\|^2_{L^2(\Omega)} \sim \sum_{j\geq j_0-1}^{\infty} \sum_{k\in\nabla_j} |(v, \psi_{j,k})_{L^2(\Omega)}|^2 \sim \sum_{j\geq j_0-1}^{\infty} \sum_{k\in\nabla_j} |(v, \widetilde{\psi}_{j,k})_{L^2(\Omega)}|^2.$$

We refer to [6] for further details.

For the construction of multiresolution bases on domains and manifolds one is interested in the *filter coefficients* or *mask coefficients* associated with the scaling functions and the wavelets. Since additional boundary functions are introduced, these filter coefficients are not fixed like in the stationary case. Therefore, we compute the full *two scale relations*

$$\Phi_j = \Phi_{j+1}\mathbf{M}_{j,0}, \quad \Psi_j = \Phi_{j+1}\mathbf{M}_{j,1},$$

and likewise for the dual counterparts

$$\widetilde{\Phi}_j = \widetilde{\Phi}_{j+1}\widetilde{\mathbf{M}}_{j,0}, \qquad \widetilde{\Psi}_j = \widetilde{\Phi}_{j+1}\widetilde{\mathbf{M}}_{j,1}.$$

We mention that these matrices will be banded and only the filter coefficients for some specific scaling functions and wavelets have to be modified. That way, the advantages of the stationary and shift-invariant case are preserved as far as possible.

1.2 Biorthogonal spline multiresolution on the interval

Our approach is based on the biorthogonal spline multiresolution on $\mathbb{R}$ developed by A. Cohen, I. Daubechies and J.-C. Feauveau [4]. These functions have several properties which make them favourite candidates for a wavelet Galerkin scheme discretizing boundary integral equations.

- The primal multiresolution consists of cardinal B-splines of the order d as scaling functions. Therefore, we have to deal with piecewise polynomials. This simplifies the construction of wavelet bases on manifolds and the computation of the matrix coefficients in the Galerkin matrix. They satisfy the requirements for a second compression which was introduced to get rid of logarithmic

terms in the complexity estimates. We like to point out that the primal multiresolution realizes the order of approximation d, i.e,

$$\inf_{v_j \in V_j} \|v - v_j\|_{L^2([0,1])} \lesssim 2^{-jd} \|v\|_d, \quad v \in H^d([0,1]).$$

- The dual multiresolution is generated by compactly supported scaling functions realizing a certain order of approximation $\widetilde{d}$ ($d + \widetilde{d}$ even). This is not of such importance as in signal analysis, because the dual bases can be avoided in the actual computations since the Galerkin method requires the adjoint and not the dual of the wavelet transform. Nevertheless, there are several situations where the inverse wavelet transform is a very helpful tool, too.

With the aid of these scaling functions, we obtain refinable spaces $V_j^{[0,1]}$ and $\widetilde{V}_j^{[0,1]}$ which contain all polynomials of degree less than d and $\widetilde{d}$, respectively. The spaces $W_j^{[0,1]}$ and $\widetilde{W}_j^{[0,1]}$ are defined uniquely via (4). Biorthogonal wavelet bases

$$\Psi_j^{[0,1]} = \left\{\psi_{j,k}^{[0,1]} : k \in \nabla_j^{[0,1]}\right\}, \quad \widetilde{\Psi}_j^{[0,1]} = \left\{\widetilde{\psi}_{j,k}^{[0,1]} : k \in \nabla_j^{[0,1]}\right\},$$

generating these complementary spaces, i.e.,

$$W_j^{[0,1]} := \operatorname{span}\left\{\Psi_j^{[0,1]}\right\}, \qquad \widetilde{W}_j^{[0,1]} := \operatorname{span}\left\{\widetilde{\Psi}_j^{[0,1]}\right\}, \tag{5}$$

are not determined uniquely. Each pair of matrices $\mathbf{M}_{j,1}^{[0,1]}, \widetilde{\mathbf{M}}_{j,1}^{[0,1]} \in \mathbb{R}^{|\Delta_{j+1}^{[0,1]}| \times |\nabla_j^{[0,1]}|}$ satisfying

$$\begin{bmatrix} \mathbf{M}_{j,0}^{[0,1]} & \mathbf{M}_{j,1}^{[0,1]} \end{bmatrix}^T \begin{bmatrix} \widetilde{\mathbf{M}}_{j,0}^{[0,1]} & \widetilde{\mathbf{M}}_{j,1}^{[0,1]} \end{bmatrix} = \mathbf{I}.$$

defines wavelets with (5) via

$$\Psi_j^{[0,1]} = \Phi_{j+1}^{[0,1]} \mathbf{M}_{j,1}^{[0,1]}, \qquad \widetilde{\Psi}_j^{[0,1]} = \widetilde{\Phi}_{j+1}^{[0,1]} \widetilde{\mathbf{M}}_{j,1}^{[0,1]}. \tag{6}$$

But, for instance, this straightforward construction does not imply fixed and finite masks in the two scale relations of the collections $\Psi_j^{[0,1]}$ and $\widetilde{\Psi}_j^{[0,1]}$. Hence, in order to define suitable wavelet bases we utilize the concept of the *stable completion* [3]. This concept is universal and often employed in the sequel but to avoid confusion we add the suffix $[0,1]$.

Definition 1.1. *Let* $\breve{\Psi}_j^{[0,1]} = \left\{\breve{\psi}_{j,k}^{[0,1]} : k \in \nabla_j^{[0,1]}\right\} \subset V_{j+1}^{[0,1]}$ *be a given collection of functions satisfying*

$$\breve{\Psi}_j^{[0,1]} = \Phi_{j+1}^{[0,1]} \breve{\mathbf{M}}_{j,1}^{[0,1]}, \qquad \breve{\mathbf{M}}_{j,1}^{[0,1]} \in \mathbb{R}^{|\Delta_{j+1}^{[0,1]}| \times |\nabla_j^{[0,1]}|},$$

such that $\begin{bmatrix}\mathbf{M}_{j,0}^{[0,1]} & \breve{\mathbf{M}}_{j,1}^{[0,1]}\end{bmatrix}$ *is invertible. We define the matrix* $\begin{bmatrix}\mathbf{G}_{j,0}^{[0,1]} & \mathbf{G}_{j,1}^{[0,1]}\end{bmatrix}$ *with* $\mathbf{G}_{j,0}^{[0,1]} \in \mathbb{R}^{|\Delta_{j+1}^{[0,1]}|\times|\Delta_j^{[0,1]}|}$ *and* $\mathbf{G}_{j,1}^{[0,1]} \in \mathbb{R}^{|\Delta_{j+1}^{[0,1]}|\times|\nabla_j^{[0,1]}|}$ *as the inverse of* $\begin{bmatrix}\mathbf{M}_{j,0}^{[0,1]} & \breve{\mathbf{M}}_{j,1}^{[0,1]}\end{bmatrix}^T$, *i.e.,*

$$\begin{bmatrix}\mathbf{M}_{j,0}^{[0,1]} & \breve{\mathbf{M}}_{j,1}^{[0,1]}\end{bmatrix}^T \begin{bmatrix}\mathbf{G}_{j,0}^{[0,1]} & \mathbf{G}_{j,1}^{[0,1]}\end{bmatrix} = \mathbf{I}. \tag{7}$$

The collection $\breve{\Psi}_j^{[0,1]}$ *is called a stable completion of* $\Phi_j^{[0,1]}$ *if*

$$\left\|\begin{bmatrix}\mathbf{M}_{j,0}^{[0,1]} & \breve{\mathbf{M}}_{j,1}^{[0,1]}\end{bmatrix}\right\|_{l^2(\Delta_{j+1}^{[0,1]})} \sim \left\|\begin{bmatrix}\mathbf{G}_{j,0}^{[0,1]} & \mathbf{G}_{j,1}^{[0,1]}\end{bmatrix}\right\|_{l^2(\Delta_{j+1}^{[0,1]})} \sim 1. \tag{8}$$

The stable completion is projected onto $W_j^{[0,1]}$ in order to get the desired primal wavelet basis, cf. [8]. In terms of the refinement matrices, the matrix $\mathbf{M}_{j,1}^{[0,1]}$ is defined by

$$\mathbf{M}_{j,1}^{[0,1]} = \left[\mathbf{I} - \mathbf{M}_{j,0}^{[0,1]}\big(\widetilde{\mathbf{M}}_{j,0}^{[0,1]}\big)^T\right]\breve{\mathbf{M}}_{j,1}^{[0,1]} =: \breve{\mathbf{M}}_{j,1}^{[0,1]} - \mathbf{M}_{j,0}^{[0,1]}\mathbf{L}_j^{[0,1]}. \tag{9}$$

One readily verifies that the matrix $\mathbf{L}_j^{[0,1]} \in \mathbb{R}^{|\Delta_j^{[0,1]}|\times|\nabla_j^{[0,1]}|}$ satisfies

$$\mathbf{L}_j^{[0,1]} = \big(\widetilde{\mathbf{M}}_{j,0}^{[0,1]}\big)^T\breve{\mathbf{M}}_{j,1}^{[0,1]} = \big(\widetilde{\Phi}_j^{[0,1]}, \breve{\Psi}_j^{[0,1]}\big)_{L^2([0,1])}. \tag{10}$$

Moreover, one concludes from the identity

$$\begin{aligned}\mathbf{I} &= \begin{bmatrix}\mathbf{M}_{j,0}^{[0,1]} & \mathbf{M}_{j,1}^{[0,1]}\end{bmatrix}^T \begin{bmatrix}\widetilde{\mathbf{M}}_{j,0}^{[0,1]} & \widetilde{\mathbf{M}}_{j,1}^{[0,1]}\end{bmatrix} \\ &= \begin{bmatrix}\mathbf{I} & -\mathbf{L}_j^{[0,1]} \\ \mathbf{0} & \mathbf{I}\end{bmatrix}^T \begin{bmatrix}\mathbf{M}_{j,0}^{[0,1]} & \breve{\mathbf{M}}_{j,1}^{[0,1]}\end{bmatrix}^T \begin{bmatrix}\mathbf{G}_{j,0}^{[0,1]} & \mathbf{G}_{j,1}^{[0,1]}\end{bmatrix} \begin{bmatrix}\mathbf{I} & \mathbf{0} \\ \big(\mathbf{L}_j^{[0,1]}\big)^T & \mathbf{I}\end{bmatrix}\end{aligned}$$

the equality

$$\begin{bmatrix}\widetilde{\mathbf{M}}_{j,0}^{[0,1]} & \widetilde{\mathbf{M}}_{j,1}^{[0,1]}\end{bmatrix} = \begin{bmatrix}\mathbf{G}_{j,0}^{[0,1]} + \mathbf{G}_{j,1}^{[0,1]}\big(\mathbf{L}_j^{[0,1]}\big)^T & \mathbf{G}_{j,1}^{[0,1]}\end{bmatrix},$$

i.e., $\widetilde{\mathbf{M}}_{j,1}^{[0,1]} = \mathbf{G}_{j,1}^{[0,1]}$.

Remark 1.2. *The definition of* $\mathbf{M}_{j,1}^{[0,1]}$ *implies*

$$\Psi_j^{[0,1]} = \Phi_{j+1}^{[0,1]}\mathbf{M}_{j,1}^{[0,1]} = \Phi_{j+1}^{[0,1]}\breve{\mathbf{M}}_{j,1}^{[0,1]} - \Phi_{j+1}^{[0,1]}\breve{\mathbf{M}}_{j,0}^{[0,1]}\mathbf{L}_j^{[0,1]} = \breve{\Psi}_j^{[0,1]} - \Phi_j^{[0,1]}\mathbf{L}_j^{[0,1]}.$$

Consequently, similarly to [31], the wavelets $\Psi_j^{[0,1]}$ *are obtained by updating* $\breve{\Psi}_j^{[0,1]}$ *by linear combinations of the coarse level generators* $\Phi_j^{[0,1]}$.

We abbreviate

$$\Psi_{j_0-1}^{[0,1]} := \Phi_{j_0}^{[0,1]}, \qquad \widetilde{\Psi}_{j_0-1}^{[0,1]} := \widetilde{\Phi}_{j_0}^{[0,1]}, \qquad \nabla_{j_0-1}^{[0,1]} = \Delta_{j_0-1}^{[0,1]},$$

and define the collections

$$\Psi^{[0,1]} = \bigcup_{j\geq j_0-1} \Psi_j^{[0,1]}, \qquad \widetilde{\Psi}^{[0,1]} = \bigcup_{j\geq j_0-1} \widetilde{\Psi}_j^{[0,1]}.$$

Then, according to [8] the following statements hold.

- The collections $\Psi^{[0,1]}$ and $\widetilde{\Psi}^{[0,1]}$ define biorthogonal Riesz bases in $L^2([0,1])$.
- The functions contained in the collections $\Psi^{[0,1]}$ and $\widetilde{\Psi}^{[0,1]}$ have $\widetilde{d}$ and d vanishing moments, respectively. That is

  $$\int_0^1 x^\alpha \psi_{j,k}(x)dx = 0, \quad \alpha = 0, 1, \ldots, \widetilde{d}-1,$$

  and likewise for the duals.
- The functions of the collections $\Psi^{[0,1]}$ and $\widetilde{\Psi}^{[0,1]}$ have the same regularity as the biorthogonal spline wavelets in $L^2(\mathbb{R})$ [33]. Therefore, the norm equivalences are valid in the same ranges, i.e.,

  $$\begin{aligned} \|v\|^2_{H^s([0,1])} &\sim \sum_{j\geq j_0-1} \sum_{k\in\nabla_j^{[0,1]}} 2^{js} \left|\left(v, \widetilde{\psi}_{j,k}^{[0,1]}\right)_{L^2([0,1])}\right|^2, \qquad s \in (-\widetilde{\gamma}, \gamma), \\ \|v\|^2_{H^s([0,1])} &\sim \sum_{j\geq j_0-1} \sum_{k\in\nabla_j^{[0,1]}} 2^{js} \left|\left(v, \psi_{j,k}^{[0,1]}\right)_{L^2([0,1])}\right|^2, \qquad s \in (-\gamma, \widetilde{\gamma}), \end{aligned} \tag{11}$$

  with γ and $\widetilde{\gamma}$ denoting the regularity of the primal and dual wavelets, respectively.

Clearly, the goal is to construct a wavelet basis such that only a few boundary wavelets do not coincide with translates and dilates of the Cohen-Daubechies-Feauveau wavelets [4]. For the treatment of boundary integral equations we focus mainly on piecewise constant and linear wavelets, i.e., $d = 1$ and $d = 2$. On the level j, we consider the interval $[0, 1]$ subdivided into 2^j equidistant subintervals. Then, of course, $V_j^{[0,1]}$ is the space generated by 2^j and $2^j + 1$ piecewise constant and linear scaling functions, respectively. The Haar basis and the hierarchical basis on the given partitioning define suitable stable completions. Unfortunately, the general situation is not that simple since we have to modify the boundary functions. For the sake of brevity we refer to [8, 21] for the details.

The discretization of the hypersingular operator requires globally continuous piecewise linear wavelet bases. According to [14, 21], for their construction, both the

scaling functions and the stable completion are required to satisfy certain boundary conditions. The scaling functions $\Phi_j^{[0,1]}$ and $\widetilde{\Phi}_j^{[0,1]}$ have to be chosen such that

$$\phi_{j,k}^{[0,1]}(0) = \begin{cases} 2^{j/2}, & k = 0, \\ 0, & k \neq 0, \end{cases} \qquad \widetilde{\phi}_{j,k}^{[0,1]}(0) = \begin{cases} 2^{j/2}c, & k = 0, \\ 0, & k \neq 0, \end{cases} \tag{12}$$

$c \neq 0$, and likewise for $x = 1$ and $k = 2^j + 1$. This is performed by a suitable change of bases. Additionally, the stable completion $\breve{\Psi}_j^{[0,1]}$ is supposed to fulfill zero boundary conditions

$$\breve{\psi}_{j,k}^{[0,1]}(0) = \breve{\psi}_{j,k}^{[0,1]}(1) = 0, \quad k \in \nabla_j^{[0,1]}, \tag{13}$$

as well as the symmetry conditions

$$\breve{\psi}_{j,k}^{[0,1]}(x) = \breve{\psi}_{j,3\cdot 2^j+1-k}^{[0,1]}(1-x), \quad x \in [0,1], \quad k \in \nabla_j^{[0,1]}. \tag{14}$$

For example, the hierarchical basis satisfies the latter conditions.

1.3 Wavelets on the unit square

In general, it suffices to consider two dimensional wavelets for the treatment of boundary integral equations. Hence, we restrict ourselves to the two dimensional case since the construction keeps simple. For the higher dimensional case we refer to [21].

1.3.1 Biorthogonal scaling functions

The canonical definition of biorthogonal multiresolutions on the unit square is to take tensor products of the univariate constructions. Hence, the collections of scaling functions are given by

$$\Phi_j^{\square} = \Phi_j^{[0,1]} \otimes \Phi_j^{[0,1]}, \qquad \widetilde{\Phi}_j^{\square} = \widetilde{\Phi}_j^{[0,1]} \otimes \widetilde{\Phi}_j^{[0,1]}, \tag{15}$$

with the index set $\Delta_j^{\square} = \Delta_j^{[0,1]} \times \Delta_j^{[0,1]}$. Consequently, the associated refinement matrices are

$$\mathbf{M}_{j,0}^{\square} = \mathbf{M}_{j,0}^{[0,1]} \otimes \mathbf{M}_{j,0}^{[0,1]}, \qquad \widetilde{\mathbf{M}}_{j,0}^{\square} = \widetilde{\mathbf{M}}_{j,0}^{[0,1]} \otimes \widetilde{\mathbf{M}}_{j,0}^{[0,1]}. \tag{16}$$

As an immediate consequence of the univariate case, the spaces $V_j^{\square} := \operatorname{span}\left\{\Phi_j^{\square}\right\}$ and $\widetilde{V}_j^{\square} := \operatorname{span}\left\{\widetilde{\Phi}_j^{\square}\right\}$ are nested and dense in $L^2(\square)$. Clearly, these spaces are exact of the order d and $\widetilde{d}$, respectively. We emphasize that the complement spaces $W_j^{\square}$ and $\widetilde{W}_j^{\square}$ are uniquely determined by (4). With this in mind, the remainder of this subsection is dedicated to the construction of biorthogonal wavelet bases $\Psi_j^{\square}$ and $\widetilde{\Psi_j^{\square}}$ with $W_j^{\square} := \operatorname{span}\left\{\Psi_j^{\square}\right\}$ and $\widetilde{W}_j^{\square} := \operatorname{span}\left\{\widetilde{\Psi}_j^{\square}\right\}$.

1.3.2 Tensor product wavelets

First, we introduce the simplest construction, namely tensor product wavelets

$$\Psi_j^{\square} = \left\{\Phi_j^{[0,1]} \otimes \Psi_j^{[0,1]}\right\} \cup \left\{\Psi_j^{[0,1]} \otimes \Phi_j^{[0,1]}\right\} \cup \left\{\Psi_j^{[0,1]} \otimes \Psi_j^{[0,1]}\right\}.$$

Then, the refinement matrices are defined via

$$\mathbf{M}_{j,1}^{\square} = \begin{bmatrix} \mathbf{M}_{j,0}^{[0,1]} \otimes \mathbf{M}_{j,1}^{[0,1]} \\ \mathbf{M}_{j,1}^{[0,1]} \otimes \mathbf{M}_{j,0}^{[0,1]} \\ \mathbf{M}_{j,1}^{[0,1]} \otimes \mathbf{M}_{j,1}^{[0,1]} \end{bmatrix}, \quad \widetilde{\mathbf{M}}_{j,1}^{\square} = \begin{bmatrix} \widetilde{\mathbf{M}}_{j,0}^{[0,1]} \otimes \widetilde{\mathbf{M}}_{j,1}^{[0,1]} \\ \widetilde{\mathbf{M}}_{j,1}^{[0,1]} \otimes \widetilde{\mathbf{M}}_{j,0}^{[0,1]} \\ \widetilde{\mathbf{M}}_{j,1}^{[0,1]} \otimes \widetilde{\mathbf{M}}_{j,1}^{[0,1]} \end{bmatrix}.$$

Hence, we differ three types of wavelets on $\square$, cf. figures 1 and 2. The first type is the tensor product $\phi_{j,k_1}^{[0,1]} \otimes \psi_{j,k_2}^{[0,1]}$. The second type is the tensor product of $\psi_{j,k_1}^{[0,1]} \otimes \phi_{j,k_2}^{[0,1]}$. The third type consists of the tensor product of two wavelets $\psi_{j,k_1}^{[0,1]} \otimes \phi_{j,k_2}^{[0,1]}$. We mention that $|\Delta_j^{[0,1]}| \approx |\nabla_j^{[0,1]}|$ implies nearly identical cardinalities of the three types of wavelets.

1.3.3 Simplified tensor product wavelets

Next, we consider an extension of the tensor product construction. As we will see it replaces the wavelet of the third type by a smoother one. We mention that this simplifies numerical integration, for instance in the Galerkin scheme.

The idea is to construct a suitable stable completion on the unit square. Based on the univariate case it can be defined by the collection

$$\breve{\Psi}_j^{\square} = \left\{\Phi_j^{[0,1]} \otimes \breve{\Psi}_j^{[0,1]}\right\} \cup \left\{\breve{\Psi}_j^{[0,1]} \otimes \Phi_j^{[0,1]}\right\} \cup \left\{\breve{\Psi}_j^{[0,1]} \otimes \breve{\Psi}_j^{[0,1]}\right\}.$$

The refinement matrices $\breve{\mathbf{M}}_{j,1}^{\square}$, $\mathbf{G}_{j,0}^{\square}$ and $\mathbf{G}_{j,1}^{\square}$ are computed by

$$\breve{\mathbf{M}}_{j,1}^{\square} = \begin{bmatrix} \mathbf{M}_{j,0}^{[0,1]} \otimes \breve{\mathbf{M}}_{j,1}^{[0,1]} \\ \breve{\mathbf{M}}_{j,1}^{[0,1]} \otimes \mathbf{M}_{j,0}^{[0,1]} \\ \breve{\mathbf{M}}_{j,1}^{[0,1]} \otimes \breve{\mathbf{M}}_{j,1}^{[0,1]} \end{bmatrix}, \qquad \mathbf{G}_{j,0}^{\square} = \mathbf{G}_{j,0}^{[0,1]} \otimes \mathbf{G}_{j,0}^{[0,1]}, \qquad \mathbf{G}_{j,1}^{\square} = \begin{bmatrix} \mathbf{G}_{j,0}^{[0,1]} \otimes \mathbf{G}_{j,1}^{[0,1]} \\ \mathbf{G}_{j,1}^{[0,1]} \otimes \mathbf{G}_{j,0}^{[0,1]} \\ \mathbf{G}_{j,1}^{[0,1]} \otimes \mathbf{G}_{j,1}^{[0,1]} \end{bmatrix}.$$

Next, the matrix $\mathbf{L}_j^{\square}$ is given by

$$\mathbf{L}_j^{\square} = \begin{bmatrix} \mathbf{I}^{(|\Delta_j^{[0,1]}|)} \otimes \mathbf{L}_j^{[0,1]} \\ \mathbf{L}_j^{[0,1]} \otimes \mathbf{I}^{(|\Delta_j^{[0,1]}|)} \\ \mathbf{L}_j^{[0,1]} \otimes \mathbf{L}_j^{[0,1]} \end{bmatrix}.$$

This implies

$$\begin{aligned} \mathbf{M}_{j,1}^{\square} &= \breve{\mathbf{M}}_{j,1}^{\square} - \mathbf{M}_{j,0}^{\square}\mathbf{L}_j^{\square} \\ &= \begin{bmatrix} \mathbf{M}_{j,0}^{[0,1]} \otimes \mathbf{M}_{j,1}^{[0,1]} \\ \mathbf{M}_{j,1}^{[0,1]} \otimes \mathbf{M}_{j,0}^{[0,1]} \\ \breve{\mathbf{M}}_{j,1}^{[0,1]} \otimes \breve{\mathbf{M}}_{j,1}^{[0,1]} - \left(\mathbf{M}_{j,0}^{[0,1]} \otimes \mathbf{M}_{j,0}^{[0,1]}\right)\left(\mathbf{L}_j^{[0,1]} \otimes \mathbf{L}_j^{[0,1]}\right) \end{bmatrix}. \end{aligned}$$

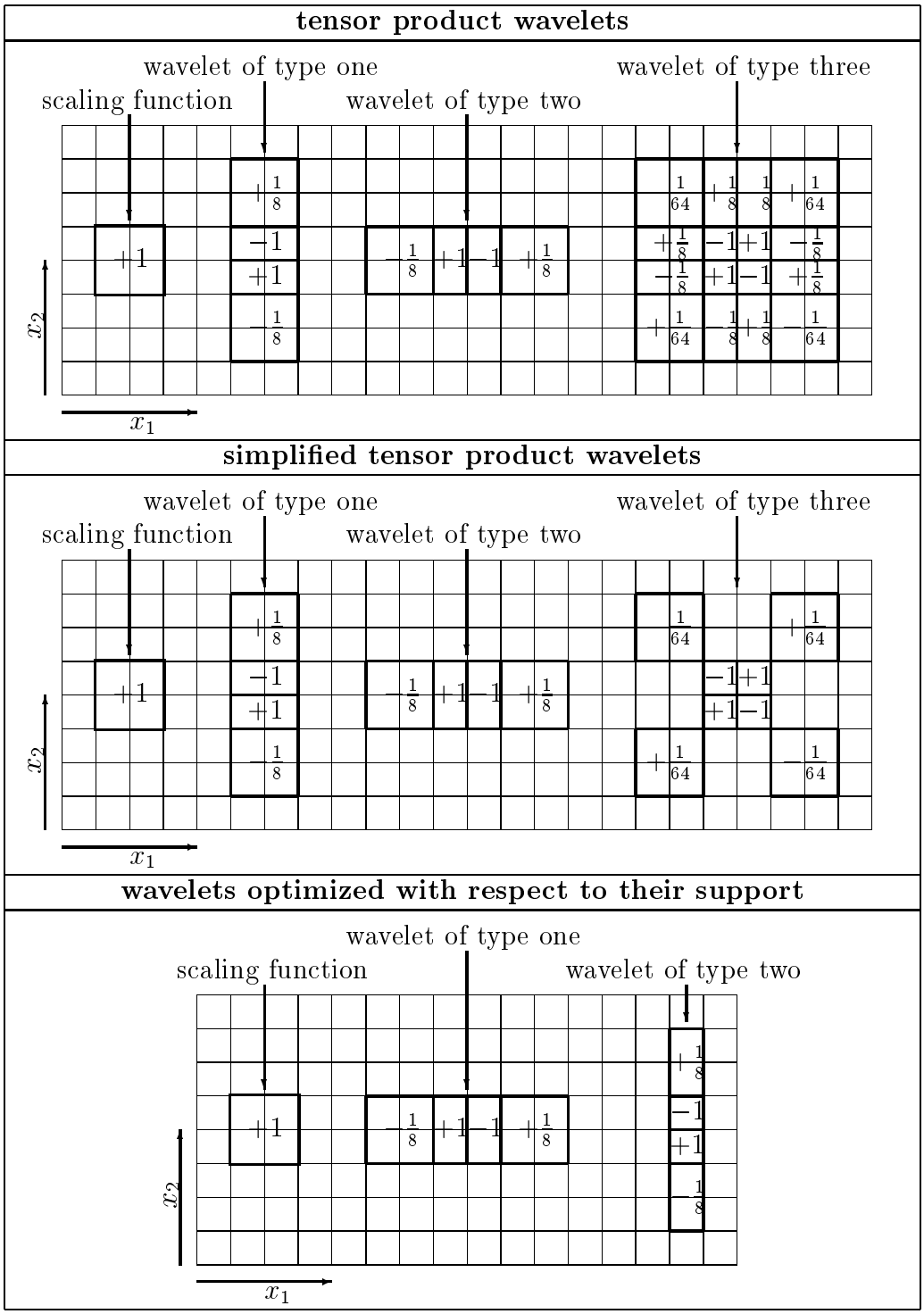

Figure 1: Interior piecewise constant wavelets with three vanishing moments. The boundary wavelets are not plotted.

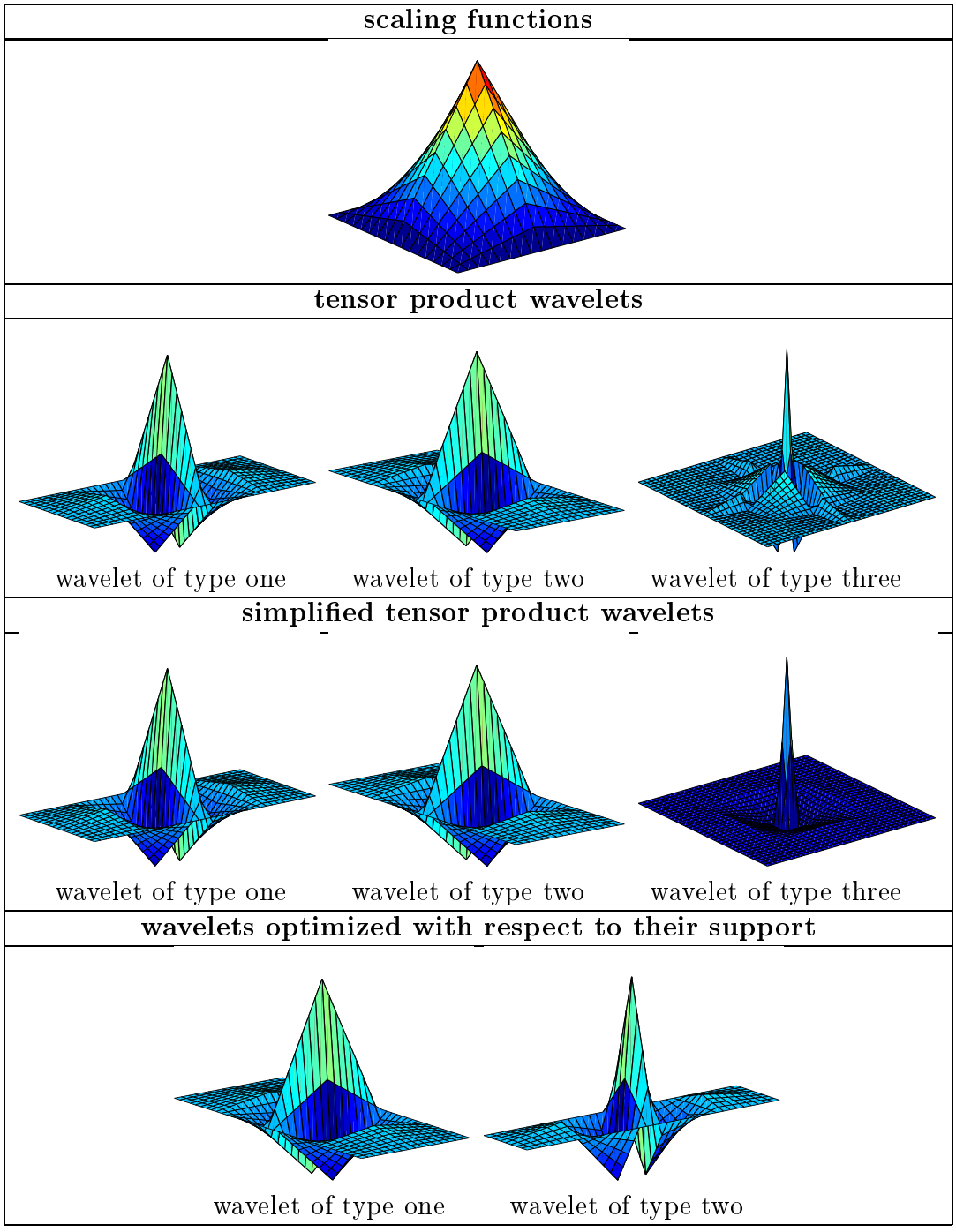

Figure 2: Interior piecewise linear wavelets with four vanishing moments. The boundary wavelets are not plotted.

Hence, we differ again three types of wavelets on $\square$. The first and the second type coincide with the tensor product wavelets, see figures 1 and 2. But now the third type consists of the tensor product of the stable completion $\breve{\psi}_{j,k_1}^{[0,1]} \otimes \breve{\psi}_{j,k_2}^{[0,1]}$ and certain scaling functions $\phi_{j,\mathbf{k}'}^{\square} = \phi_{j,k_1'}^{[0,1]} \otimes \phi_{j,k_2'}^{[0,1]}$ of the coarse grid j. In general, the support of this wavelet does not depend on the choice of the stable completion. But choosing a stable completion on $[0,1]$ with small supports, the product $\breve{\psi}_{j,k_1}^{[0,1]} \otimes \breve{\psi}_{j,k_2}^{[0,1]} \in V_{j+1}^{\square}$ has also small support. Since the additional scaling functions belong to $V_j^{\square}$, the wavelet is smoother than the corresponding tensor product wavelet.

1.3.4 Wavelets optimized with respect to their supports

Last, we consider a more advanced construction which yields wavelets with very small supports. We define the wavelet functions via the collections

$$\begin{aligned}\Psi_j^{\square} &= \left\{\Psi_j^{[0,1]} \otimes \Phi_j^{[0,1]}\right\} \cup \left\{\Phi_{j+1}^{[0,1]} \otimes \Psi_j^{[0,1]}\right\},\\ \widetilde{\Psi}_j^{\square} &= \left\{\widetilde{\Psi}_j^{[0,1]} \otimes \widetilde{\Phi}_j^{[0,1]}\right\} \cup \left\{\widetilde{\Phi}_{j+1}^{[0,1]} \otimes \widetilde{\Psi}_j^{[0,1]}\right\}.\end{aligned}$$

The refinement matrices $\mathbf{M}_{j,1}^{\square}$ and $\widetilde{\mathbf{M}}_{j,1}^{\square}$ are computed by

$$\mathbf{M}_{j,1}^{\square} = \begin{bmatrix} \mathbf{M}_{j,1}^{[0,1]} \otimes \mathbf{M}_{j,0}^{[0,1]} \\ \mathbf{I}^{|\Delta_{j+1}^{[0,1]}|} \otimes \mathbf{M}_{j,1}^{[0,1]} \end{bmatrix}, \qquad \widetilde{\mathbf{M}}_{j,1}^{\square} = \begin{bmatrix} \widetilde{\mathbf{M}}_{j,1}^{[0,1]} \otimes \widetilde{\mathbf{M}}_{j,0}^{[0,1]} \\ \mathbf{I}^{|\Delta_{j+1}^{[0,1]}|} \otimes \widetilde{\mathbf{M}}_{j,1}^{[0,1]} \end{bmatrix}.$$

Thus, we obtain two types of wavelets on $\square$, cf. figures 1 and 2. The first type is the tensor product $\psi_{j,k_1}^{[0,1]} \otimes \phi_{j,k_2}^{[0,1]}$. The second type is the tensor product $\phi_{j+1,k_1}^{[0,1]} \otimes \psi_{j,k_2}^{[0,1]}$. Notice that these wavelets have a very small support in comparison with the previously introduced wavelets, since a scaling function of the fine grid $j+1$ appears in the first coordinate. Additionally, the number of wavelets of type two is nearly twice as much as the number of wavelets of type one.

Remark 1.3. *This construction is highly attractive in higher dimensions since each wavelet coincides only in one coordinate with a wavelet from the interval while in the other coordinates only scaling functions of the levels j and $j+1$ appear.*

1.4 Wavelets on domains and manifolds

In this subsection, we employ a domain decomposition strategy and introduce a family of parametric representations which describe the given manifold. Subsequently, the wavelets on the manifold are defined via the parametrization. We consider two different constructions for wavelets on manifolds. The first one leads to wavelets which are defined on each patch individually. The second and more complicated one yields globally continuous wavelets.

1.4.1 Parametric representations of manifolds

Let $\square$ denote the unit square, i. e., $\square = [0,1]^2$. We subdivide the given manifold $\Gamma \in \mathbb{R}^3$ into several *patches*

$$\Gamma = \bigcup_{i=1}^{N} \Gamma_i, \qquad \Gamma_i = \gamma_i(\square), \qquad i = 1, 2, \ldots, N, \tag{17}$$

such that each $\gamma_i : \square \to \Gamma_i$ defines a diffeomorphism of $\square$ onto Γ_i. The intersection $\Gamma_i \cap \Gamma_{i'}$, $i \neq i'$, of the patches Γ_i and $\Gamma_{i'}$ is supposed to be either $\emptyset$ or a common edge or vertex. On the level j, the unit square is subdivided equidistantly j times into 2^{2j} squares $C_{j,\mathbf{k}} \subseteq \square$, where $\mathbf{k} = (k_1, k_2)$ with $0 \leq k_m < 2^j$. This yields $2^{2j}N$ *elements* $\Gamma_{i,j,\mathbf{k}} := \gamma_i(C_{j,\mathbf{k}}) \subseteq \Gamma_i$, $i = 1, 2, \ldots, N$. The construction of globally continuous wavelets requires additionally that the collection of all elements $\{\Gamma_{i,j,\mathbf{k}}\}$ on a fixed level j forms a regular mesh on Γ. Therefore, the parametric representation is subjected the following matching condition. For all $\mathbf{x} \in \Gamma_i \cap \Gamma_{i'}$ exists a bijective, affine mapping $\Xi : \square \to \square$ such that $\gamma_i(\mathbf{s}) = (\gamma_{i'} \circ \Xi)(\mathbf{s}) = \mathbf{x}$ for $\mathbf{s} = [s_1, s_2]^T \in \square$ with $\gamma_i(\mathbf{s}) = \mathbf{x}$, cf. figure 3. Unfortunately, this essential supposition restricts the choice of the parametric representation.

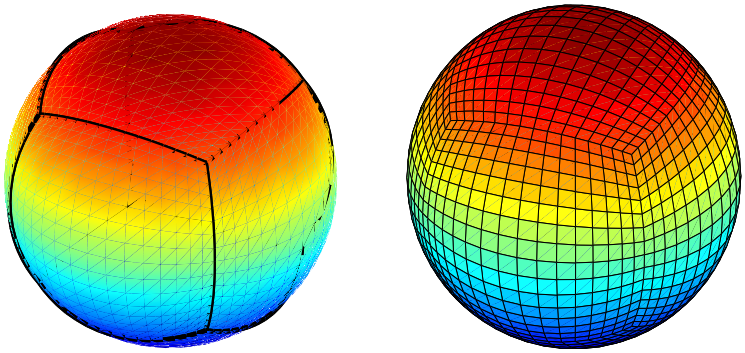

Figure 3: The parametric representation of the unit sphere is obtained by projecting it onto the cube $[-1,1]^3$, which yields six patches (left). On the right hand side one figures out the partition on the level $j = 4$.

The first fundamental tensor of differential geometry is given by the matrix $\mathbf{K}_i(\mathbf{s}) \in \mathbb{R}^{2\times 2}$ with

$$\mathbf{K}_i(\mathbf{s}) := \Big[\Big(\frac{\partial \gamma_i(\mathbf{s})}{\partial s_j}, \frac{\partial \gamma_{i'}(\mathbf{s})}{\partial s_{j'}}\Big)_{l^2(\mathbb{R}^3)}\Big]_{j,j'=1,2}. \tag{18}$$

Since γ_i is supposed to be a diffeomorphism, the matrix $\mathbf{K}_i(\mathbf{s})$ is symmetric and positive definite. The canonical inner product in $L^2(\Gamma)$ is given by

$$(u,v)_{L^2(\Gamma)} = \int_\Gamma u(\mathbf{x})v(\mathbf{x})d\sigma_{\mathbf{x}} = \sum_{i=1}^N \int_\square u\big(\gamma_i(\mathbf{s})\big)v\big(\gamma_i(\mathbf{s})\big)\sqrt{\det\big(\mathbf{K}_i(\mathbf{s})\big)}d\mathbf{s}. \tag{19}$$

The corresponding Sobolev spaces are indicated by $H^s(\Gamma)$. Of course, depending on the global smoothness of the surface, the range of permitted $s \in \mathbb{R}$ is limited to $s \in (-s_\Gamma, s_\Gamma)$. An important role is played by the following modified inner product which arises from (19) by omitting the square root of $\det\big(\mathbf{K}_i(\mathbf{s})\big)$

$$\langle u,v\rangle = \sum_{i=1}^N (u\circ\gamma_i, v\circ\gamma_i)_{L^2(\square)} = \sum_{i=1}^N \int_\square u\big(\gamma_i(\mathbf{s})\big)v\big(\gamma_i(\mathbf{s})\big)d\mathbf{s}. \tag{20}$$

In $L^2(\Gamma)$ both inner products define equivalent norms $\langle u,u\rangle \sim (u,u)_{L^2(\Gamma)}$. However, in general, even on smooth surfaces $\mathbf{K}_i(\mathbf{s})$ is not continuous accross the interfaces of the patches, i.e., for $\gamma_i(\mathbf{s}) = \gamma_{i'}(\mathbf{s}') = \mathbf{x} \in \Gamma_i \cap \Gamma_{i'}$ one has

$$\mathbf{K}_i(\mathbf{s}) \neq \mathbf{K}_{i'}(\mathbf{s}'). \tag{21}$$

In the next subsections, the biorthogonal multiresolution on Γ is constructed with respect to the modified inner product. Thus, due to (21), the norm equivalence with respect to the canonical Sobolev spaces $H^s(\Gamma)$ is limited from below by $s = -1/2$.

1.4.2 Patchwise smooth wavelet bases

If the wavelet basis is not required globally continuous, one may employ wavelet bases defined on each patch individually. This strategy reflects the canonical one for the piecewise constants. But in the case of piecewise linear functions we obtain multiple defined knots along the interfaces of intersecting patches. This leads to more degrees of freedom than in the case of global continuity.

The primal scaling functions and wavelets are given by

$$\phi_{j,\mathbf{k}}^{\Gamma_i}(\mathbf{x}) := \begin{cases} \phi_{j,\mathbf{k}}^{\square}\big(\gamma_i^{-1}(\mathbf{x})\big), & \mathbf{x}\in\Gamma_i, \\ 0, & \text{else}, \end{cases} \qquad \psi_{j,\mathbf{k}}^{\Gamma_i}(\mathbf{x}) := \begin{cases} \psi_{j,\mathbf{k}}^{\square}\big(\gamma_i^{-1}(\mathbf{x})\big), & \mathbf{x}\in\Gamma_i, \\ 0, & \text{else}. \end{cases}$$

Setting $\Phi_j^{\Gamma_i} = \big\{\phi_{j,\mathbf{k}}^{\Gamma_i} : \mathbf{k}\in\Delta_j^{\square}\big\}$ and $\Psi_j^{\Gamma_i} = \big\{\psi_{j,\mathbf{k}}^{\Gamma_i} : \mathbf{k}\in\nabla_j^{\square}\big\}$, the collections of scaling functions and wavelets on Γ are defined by $\Phi_j^\Gamma := \big\{\Phi_j^{\Gamma_i}\big\}_{i=1}^N$ and $\Psi_j^\Gamma := \big\{\Psi_j^{\Gamma_i}\big\}_{i=1}^N$. Obviously, the refinement matrices with $\Phi_j^\Gamma = \Phi_{j+1}^\Gamma \mathbf{M}_{j,0}^\Gamma$ and $\Psi_j^\Gamma = \Phi_{j+1}^\Gamma \mathbf{M}_{j,1}^\Gamma$ are obtained by

$$\mathbf{M}_{j,0}^\Gamma = \operatorname{diag}\big(\underbrace{\mathbf{M}_{j,0}^{\square},\ldots,\mathbf{M}_{j,0}^{\square}}_{N\text{ times}}\big), \qquad \mathbf{M}_{j,1}^\Gamma = \operatorname{diag}\big(\underbrace{\mathbf{M}_{j,1}^{\square},\ldots,\mathbf{M}_{j,1}^{\square}}_{N\text{ times}}\big).$$

Clearly, the spaces $V_j^\Gamma := \operatorname{span}\{\Phi_j^\Gamma\}$ are nested. In addition, we find $V_{j+1}^\Gamma = V_j^\Gamma \oplus W_j^\Gamma$, where $W_j^\Gamma := \operatorname{span}\{\Psi_j^\Gamma\}$. Proceeding analogously on the dual side yields a multiresolution on Γ which is biorthogonal with respect to the modified inner product (20).

Analogously to the univariate case we define the collection of wavelets

$$\Psi^\Gamma = \bigcup_{j\geq j_0-1} \Psi_j^\Gamma, \qquad \widetilde{\Psi}^\Gamma = \bigcup_{j\geq j_0-1} \widetilde{\Psi}_j^\Gamma,$$

with $\Psi_{j_0-1}^\Gamma := \Phi_{j_0}^\Gamma$ and $\widetilde{\Psi}_{j_0-1}^\Gamma := \widetilde{\Phi}_{j_0}^\Gamma$. In order to formulate the properties of the wavelets we introduce new function spaces on Γ. For arbitrary $s \geq 0$ we define the Sobolev spaces $H^s_{\langle\cdot,\cdot\rangle}(\Gamma)$ as closure of all patchwise C^∞-functions on Γ with respect to the norm

$$\|v\|_{H^s_{\langle\cdot,\cdot\rangle}(\Gamma)} := \sum_{i=1}^N \|v\circ\gamma_i\|_{H^s(\square)}.$$

The space $L^2_{\langle\cdot,\cdot\rangle}(\Gamma)$ indicates as usual the Sobolev space $H^0_{\langle\cdot,\cdot\rangle}(\Gamma)$. The Sobolev spaces of negative order, that is $H^{-s}_{\langle\cdot,\cdot\rangle}(\Gamma)$, are defined as the duals of $H^s_{\langle\cdot,\cdot\rangle}(\Gamma)$ with respect to the modified inner product (20). Consequently, $H^{-s}_{\langle\cdot,\cdot\rangle}(\Gamma)$ is equipped by the norm

$$\|v\|_{H^{-s}_{\langle\cdot,\cdot\rangle}(\Gamma)} := \sup_{w\in H^s_{\langle\cdot,\cdot\rangle}(\Gamma)} \frac{\langle v,w\rangle}{\|w\|_{H^s_{\langle\cdot,\cdot\rangle}(\Gamma)}}.$$

Proposition 1.4. *The collection of wavelets Ψ^Γ and $\widetilde{\Psi}^\Gamma$ form biorthogonal Riesz bases in $L^2_{\langle\cdot,\cdot\rangle}(\Gamma)$. The primal wavelets have $\widetilde{d}$ vanishing moments in terms of*

$$\int_\square \mathbf{s}^{\boldsymbol{\alpha}} \psi_{j,\mathbf{k}}^\Gamma\big(\gamma_i(\mathbf{s})\big)d\mathbf{s} = 0, \qquad |\boldsymbol{\alpha}| < \widetilde{d}, \qquad i = 1,2,\ldots,N, \tag{22}$$

where $\boldsymbol{\alpha} = (\alpha_1,\alpha_2)$ denotes a multi index and $|\boldsymbol{\alpha}| := \alpha_1+\alpha_2$. Moreover, the norm equivalences

$$\|v\|^2_{H^s_{\langle\cdot,\cdot\rangle}(\Gamma)} \sim \sum_{j\geq j_0-1}\sum_{\mathbf{k}\in\nabla_j^\Gamma} 2^{2sj}\big|\langle v,\widetilde{\psi}_{j,\mathbf{k}}^\Gamma\rangle\big|^2, \qquad s\in(-\widetilde{\gamma},\gamma),$$

$$\|v\|^2_{H^s_{\langle\cdot,\cdot\rangle}(\Gamma)} \sim \sum_{j\geq j_0-1}\sum_{\mathbf{k}\in\nabla_j^\Gamma} 2^{2sj}\big|\langle v,\psi_{j,\mathbf{k}}^\Gamma\rangle\big|^2, \qquad s\in(-\gamma,\widetilde{\gamma}),$$

hold with γ and $\widetilde{\gamma}$ corresponding to the Cohen-Daubechies-Feauveau wavelets [4].

We remark that the Sobolev spaces $H^s(\Gamma)$ and $H^s_{\langle\cdot,\cdot\rangle}(\Gamma)$ are isomorphic in the range $s\in\big(-\frac{1}{2},\frac{1}{2}\big)$, see [14] for details. Therefore, the norm equivalences with respect to

the canonical Sobolev spaces are valid in the ranges

$$\|v\|^2_{H^s(\Gamma)} \sim \sum_{j\geq j_0-1}\sum_{\mathbf{k}\in\nabla_j^\Gamma} 2^{2sj}\big|\big(v,\widetilde{\psi}^\Gamma_{j,\mathbf{k}}\big)_{L^2(\Gamma)}\big|^2, \qquad s\in\big(-\min\big\{\tfrac{1}{2},\widetilde{\gamma}\big\},\min\big\{\tfrac{1}{2},\gamma\big\}\big),$$

$$\|v\|^2_{H^s(\Gamma)} \sim \sum_{j\geq j_0-1}\sum_{\mathbf{k}\in\nabla_j^\Gamma} 2^{2sj}\big|\big(v,\psi^\Gamma_{j,\mathbf{k}}\big)_{L^2(\Gamma)}\big|^2, \qquad s\in\big(-\min\big\{\tfrac{1}{2},\gamma\big\},\min\big\{\tfrac{1}{2},\widetilde{\gamma}\big\}\big).$$

In particular, $s=0$ implies the Riesz property of the collection Ψ^Γ and $\widetilde{\Psi}^\Gamma$, respectively.

Remark 1.5. *The moment property* (22) *implies the cancellation property with respect to both inner products. More precisely, let* $\mathcal{A}: H^q_{\langle\cdot,\cdot\rangle}(\Gamma)\to H^{-q}_{\langle\cdot,\cdot\rangle}(\Gamma)$ *denote a boundary integral operator of the order* $2q$*. Then, the estimate*

$$\big|\langle\mathcal{A}\psi^\Gamma_{j',\boldsymbol{\xi}'},\psi^\Gamma_{j,\boldsymbol{\xi}}\rangle\big| \lesssim \frac{2^{-(j+j')(\widetilde{d}+1)}}{\|\operatorname{dist}(\operatorname{supp}\psi^\Gamma_{j,\boldsymbol{\xi}},\operatorname{supp}\psi^\Gamma_{j',\boldsymbol{\xi}'})\|^{2+2\widetilde{d}+2q}} \tag{23}$$

is satisfied. Analogously, considering a boundary integral operator $\widetilde{\mathcal{A}}: H^q(\Gamma)\to H^{-q}(\Gamma)$ *of the order* $2q$ *we find*

$$\big|(\widetilde{\mathcal{A}}\psi^\Gamma_{j',\boldsymbol{\xi}'},\psi^\Gamma_{j,\boldsymbol{\xi}})_{L^2(\Gamma)}\big| \lesssim \frac{2^{-(j+j')(\widetilde{d}+1)}}{\|\operatorname{dist}(\operatorname{supp}\psi^\Gamma_{j,\boldsymbol{\xi}},\operatorname{supp}\psi^\Gamma_{j',\boldsymbol{\xi}'})\|^{2+2\widetilde{d}+2q}}. \tag{24}$$

According to [30], this cancellation property is sufficient to compress the system matrices of $\mathcal{A}$ *and* $\widetilde{\mathcal{A}}$*, for instance in a Galerkin scheme.*

1.4.3 Globally continuous piecewise linear wavelets

The construction of globally continuous piecewise linear wavelets on Γ is based on the simplified tensor product wavelets. Both, the scaling functions and the stable completion, are required to satisfy the boundary conditions. In order to perform the continuity a gluing technique is utilized along the interfaces of intersecting patches. For the sake of clearness in representation, we introduce first some further notation since we have to deal with local indices and functions defined on the parameter domain $\square$ as well as global indices and functions on the surface Γ.

To this end, it is convenient to identify the basis functions with physical grid points on the mesh on the unit square, i.e., we employ the bijective mapping

$$q_j:\Delta_j^\square\to\square, \quad q_j(\mathbf{k})=2^{-j}\mathbf{k},$$

in order to redefine our index sets on the unit square. Then, the boundary conditions (12) and (13) imply

$$\phi^\square_{j,\mathbf{k}}\Big|_{\partial\square}\equiv\widetilde{\phi}^\square_{j,\mathbf{k}}\Big|_{\partial\square}\equiv 0, \qquad \mathbf{k}\in\Delta_j^\square\cap\square^\circ,$$

$$\breve{\psi}^\square_{j,\mathbf{k}}\Big|_{\partial\square}\equiv 0, \qquad \mathbf{k}\in\nabla_j^\square\cap\square^\circ.$$

That is, all functions corresponding to the indices $\mathbf{k}$ lying in the interior of $\square$ satisfy zero boundary conditions. Moreover, given any affine mapping $\Xi : \square \to \square$, there holds

$$\Phi_j^{\square} = \Phi_j^{\square} \circ \Xi, \qquad \breve{\Psi}_j^{\square} = \breve{\Psi}_j^{\square} \circ \Xi, \qquad \widetilde{\Phi}_j^{\square} = \widetilde{\Phi}_j^{\square} \circ \Xi, \qquad \widetilde{\Psi}_j^{\square} = \widetilde{\Psi}_j^{\square} \circ \Xi. \tag{25}$$

A given point $\mathbf{x} \in \Gamma$ might have several representations

$$\mathbf{x} = \gamma_{i_1}(\mathbf{s}_1) = \ldots = \gamma_{i_{r(\mathbf{x})}}(\mathbf{s}_{r(\mathbf{x})})$$

if $\mathbf{x}$ belongs to different patches $\Gamma_{i_1}, \ldots, \Gamma_{i_{r(\mathbf{x})}}$. Of course, this occurs only if $\mathbf{x}$ lies on a common edge or vertex of these patches. We count the number of preimages to a given point $\mathbf{x} \in \Gamma$ by the function $r : \Gamma \to \mathbb{N}$,

$$r(\mathbf{x}) := \big|\big\{i \in \{1, 2, \ldots, N\} : \mathbf{x} \in \Gamma_i\big\}\big|. \tag{26}$$

Clearly, one has $r(\mathbf{x}) \geq 1$, where $r(\mathbf{x}) = 1$ holds for all $\mathbf{x}$ lying in the interior of the patches Γ_i. Moreover, $r(\mathbf{x}) = 2$ for all $\mathbf{x}$ which belong to an edge and are different from a vertex.

Next, given two points $\mathbf{x}, \mathbf{y} \in \Gamma$, the function $c : \Gamma \times \Gamma \to \mathbb{N}$ defined by

$$c(\mathbf{x}, \mathbf{y}) := \big|\big\{i \in \{1, 2, \ldots, N\} : \mathbf{x} \in \Gamma_i \wedge \mathbf{y} \in \Gamma_i\big\}\big| \tag{27}$$

counts the number of patches Γ_i containing both points together.

Now, on Γ, the index sets are given by physical grid points on the surface

$$\Delta_j^{\Gamma} := \big\{\gamma_i(\mathbf{k}) : \mathbf{k} \in \Delta_j^{\square},\ i \in \{1, 2, \ldots, N\}\big\}, \qquad \nabla_j^{\Gamma} := \Delta_{j+1}^{\Gamma} \setminus \Delta_j^{\Gamma}. \tag{28}$$

The gluing along the intersections of the patches is performed as follows. According to [14], the scaling functions $\Phi_j^{\Gamma} := \big\{\phi_{j,\boldsymbol{\xi}}^{\Gamma} : \boldsymbol{\xi} \in \Delta_j^{\Gamma}\big\}$ and $\widetilde{\Phi}_j^{\Gamma} := \big\{\widetilde{\phi}_{j,\boldsymbol{\xi}}^{\Gamma} : \boldsymbol{\xi} \in \Delta_j^{\Gamma}\big\}$ are defined by

$$\begin{aligned}
\phi_{j,\boldsymbol{\xi}}^{\Gamma}(\mathbf{x}) &= \begin{cases} \phi_{j,\mathbf{k}}^{\square}\big(\gamma_i^{-1}(\mathbf{x})\big), & \exists (i,\mathbf{k}) : \gamma_i(\mathbf{k}) = \boldsymbol{\xi} \wedge \mathbf{x} \in \Gamma_i, \\ 0, & \text{elsewhere.} \end{cases} \\
\widetilde{\phi}_{j,\boldsymbol{\xi}}^{\Gamma}(\mathbf{x}) &= \begin{cases} \frac{1}{r(\boldsymbol{\xi})}\widetilde{\phi}_{j,\mathbf{k}}^{\square}\big(\gamma_i^{-1}(\mathbf{x})\big), & \exists (i,\mathbf{k}) : \gamma_i(\mathbf{k}) = \boldsymbol{\xi} \wedge \mathbf{x} \in \Gamma_i, \\ 0, & \text{elsewhere.} \end{cases}
\end{aligned} \tag{29}$$

On the primal side, this definition reflects the canonical strategy. On the dual side, the strategy is analogously except for normalization, see also figure 4. The normalization factor ensures biorthogonality with respect to the modified inner product (20), i.e., $\langle \Phi_j^{\Gamma}, \widetilde{\Phi}_j^{\Gamma} \rangle = \mathbf{I}$. The scaling functions are refinable Riesz bases of the spaces $V_j^{\Gamma} := \operatorname{span}\big\{\Phi_j^{\Gamma}\big\}$ and $\widetilde{V}_j^{\Gamma} := \operatorname{span}\big\{\widetilde{\Phi}_j^{\Gamma}\big\}$.

The refinement matrices corresponding to these scaling functions

$$\Phi_j^{\Gamma} = \Phi_{j+1}^{\Gamma}\mathbf{M}_{j,0}^{\Gamma}, \qquad \widetilde{\Phi}_j^{\Gamma} = \widetilde{\Phi}_{j+1}^{\Gamma}\widetilde{\mathbf{M}}_{j,0}^{\Gamma}, \qquad \mathbf{M}_{j,0}^{\Gamma},\ \widetilde{\mathbf{M}}_{j,0}^{\Gamma} \in \mathbb{R}^{|\Delta_{j+1}^{\Gamma}| \times |\Delta_j^{\Gamma}|},$$

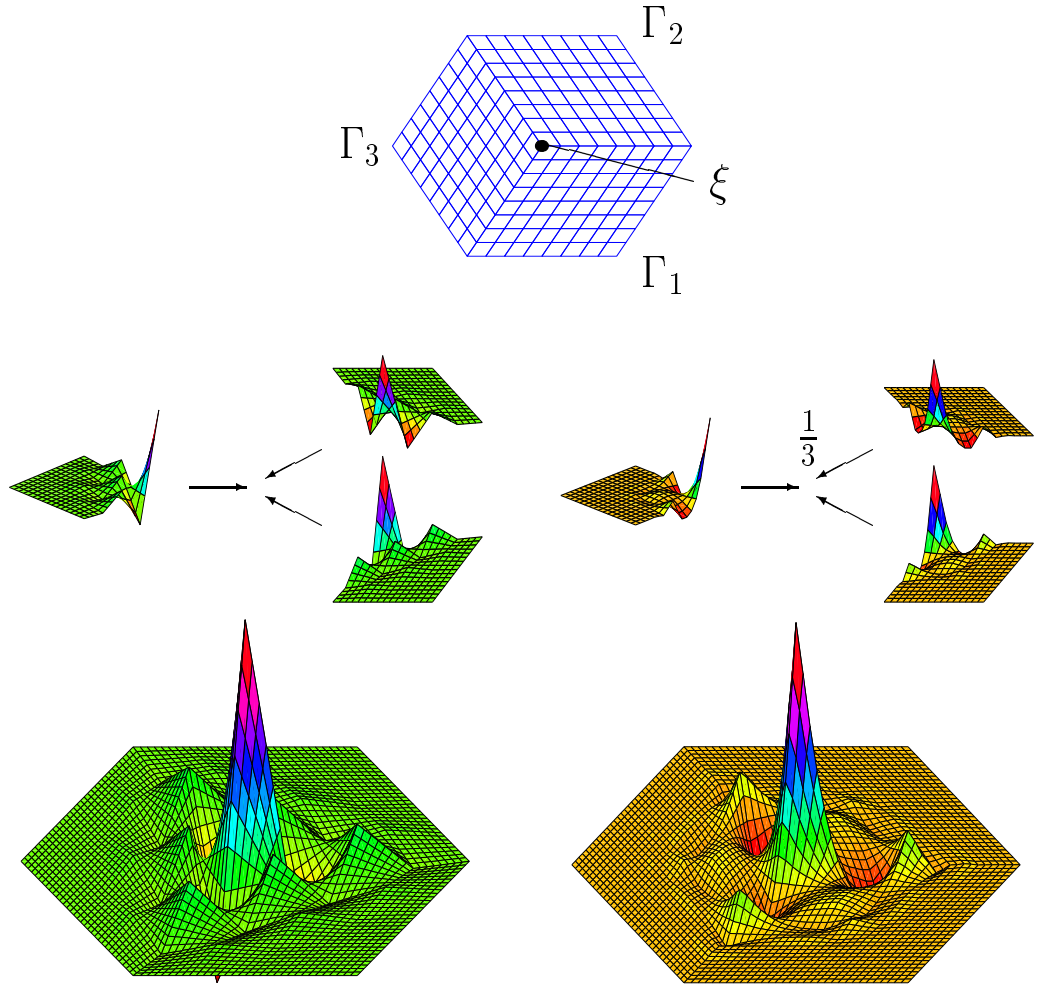

Figure 4: The primal (left) and the dual (right) generator on a degenerated vertex in the case $(d, \widetilde{d}) = (2, 4)$.

are given by

$$\left[\mathbf{M}^{\Gamma}_{j,0}\right]_{\boldsymbol{\xi}',\boldsymbol{\xi}} = \begin{cases} \left[\mathbf{M}^{\square}_{j,0}\right]_{\mathbf{k}',\mathbf{k}}, & \exists(i,\mathbf{k},\mathbf{k}') : \boldsymbol{\xi} = \gamma_i(\mathbf{k}) \wedge \boldsymbol{\xi}' = \gamma_i(\mathbf{k}'), \\ 0, & \text{elsewhere}, \end{cases} \tag{30}$$

$$\left[\widetilde{\mathbf{M}}^{\Gamma}_{j,0}\right]_{\boldsymbol{\xi}',\boldsymbol{\xi}} = \begin{cases} \frac{c(\boldsymbol{\xi},\boldsymbol{\xi}')}{r(\boldsymbol{\xi})}\left[\widetilde{\mathbf{M}}^{\square}_{j,0}\right]_{\mathbf{k}',\mathbf{k}}, & \exists(i,\mathbf{k},\mathbf{k}') : \boldsymbol{\xi} = \gamma_i(\mathbf{k}) \wedge \boldsymbol{\xi}' = \gamma_i(\mathbf{k}'), \\ 0, & \text{elsewhere}. \end{cases} \tag{31}$$

The stable completion $\breve{\Psi}_j = \left\{\breve{\psi}^{\Gamma}_{j,\boldsymbol{\xi}} : \boldsymbol{\xi} \in \nabla^{\Gamma}_j\right\}$ is defined analogously to the primal scaling functions. In accordance with [14] one has

$$\breve{\psi}^{\Gamma}_{j,\boldsymbol{\xi}}(\mathbf{x}) = \begin{cases} \breve{\psi}^{\square}_{j,\mathbf{k}}\big(\gamma_i^{-1}(\mathbf{x})\big), & \exists(i,\mathbf{k}) : \gamma_i(\mathbf{k}) = \boldsymbol{\xi} \wedge \mathbf{x} \in \Gamma_i, \\ 0, & \text{elsewhere}. \end{cases} \tag{32}$$

Consequently, the refinement matrix

$$\breve{\Psi}_j^\Gamma = \Phi_{j+1}^\Gamma \breve{\mathbf{M}}_{j,1}^\Gamma, \qquad \breve{\mathbf{M}}_{j,1}^\Gamma \in \mathbb{R}^{|\Delta_{j+1}^\Gamma| \times |\nabla_j^\Gamma|},$$

is determined analogously to $\mathbf{M}_{j,0}^\Gamma$ by

$$\left[\breve{\mathbf{M}}_{j,1}^\Gamma\right]_{\boldsymbol{\xi}',\boldsymbol{\xi}} = \begin{cases} \left[\breve{\mathbf{M}}_{j,1}^\square\right]_{\mathbf{k}',\mathbf{k}}, & \exists (i,\mathbf{k},\mathbf{k}') : \boldsymbol{\xi} = \gamma_i(\mathbf{k}) \wedge \boldsymbol{\xi}' = \gamma_i(\mathbf{k}'), \\ 0, & \text{elsewhere.} \end{cases} \tag{33}$$

The dual wavelets $\widetilde{\Psi}_j^\Gamma := \left\{\widetilde{\psi}_{j,\boldsymbol{\xi}}^\Gamma : \boldsymbol{\xi} \in \nabla_j^\Gamma\right\}$ are obtained by their refinement relation. There holds

$$\widetilde{\Psi}_j^\Gamma = \widetilde{\Phi}_{j+1}^\Gamma \widetilde{\mathbf{M}}_{j,1}^\Gamma, \qquad \widetilde{\mathbf{M}}_{j,1}^\Gamma \in \mathbb{R}^{|\Delta_{j+1}^\Gamma| \times |\nabla_j^\Gamma|},$$

with $\widetilde{\mathbf{M}}_{j,1}^\Gamma$ given by

$$\left[\widetilde{\mathbf{M}}_{j,1}^\Gamma\right]_{\boldsymbol{\xi}',\boldsymbol{\xi}} = \begin{cases} \frac{c(\boldsymbol{\xi},\boldsymbol{\xi}')}{r(\boldsymbol{\xi})} \left[\widetilde{\mathbf{M}}_{j,1}^\square\right]_{\mathbf{k}',\mathbf{k}}, & \exists (i,\mathbf{k},\mathbf{k}') : \boldsymbol{\xi} = \gamma_i(\mathbf{k}) \wedge \boldsymbol{\xi}' = \gamma_i(\mathbf{k}'), \\ 0, & \text{elsewhere,} \end{cases} \tag{34}$$

cf. [14, 21]. A closed expression of the matrix

$$\mathbf{L}_j^\Gamma := \left(\widetilde{\mathbf{M}}_{j,0}^\Gamma\right)^T \breve{\mathbf{M}}_{j,1}^\Gamma \in \mathbb{R}^{|\Delta_j^\Gamma| \times |\nabla_j^\Gamma|}$$

is crucial for the implementation of the discrete wavelet transform. In fact, the next theorem confirms the existence of an explicit formula [21].

Theorem 1.6. *The entries of the matrix* $\mathbf{L}_j^\Gamma = \left(\widetilde{\mathbf{M}}_{j,0}^\Gamma\right)^T \breve{\mathbf{M}}_{j,1}^\Gamma$ *are given by*

$$\left[\mathbf{L}_j^\Gamma\right]_{\boldsymbol{\xi}',\boldsymbol{\xi}} = \begin{cases} \frac{c(\boldsymbol{\xi},\boldsymbol{\xi}')}{r(\boldsymbol{\xi}')} \left[\mathbf{L}_j^\square\right]_{\mathbf{k}',\mathbf{k}}, & \exists (i,\mathbf{k},\mathbf{k}') : \boldsymbol{\xi} = \gamma_i(\mathbf{k}) \wedge \boldsymbol{\xi}' = \gamma_i(\mathbf{k}'), \\ 0, & \textit{elsewhere.} \end{cases} \tag{35}$$

As an immediate consequence of this theorem, a black box algorithm for the computation of the discrete wavelet transform is available. Of course, the definitions of the refinement matrices seem to be very technical. However, as the algorithms 1 and 2 confirm, the implementation of the discrete wavelet transform is rather canonical.

The collection of wavelets are given by

$$\Psi^\Gamma = \bigcup_{j \geq j_0 - 1} \Psi_j^\Gamma, \qquad \widetilde{\Psi}^\Gamma = \bigcup_{j \geq j_0 - 1} \widetilde{\Psi}_j^\Gamma,$$

with $\Psi_{j_0-1}^\Gamma := \Phi_{j_0}^\Gamma$ and $\widetilde{\Psi}_{j_0-1}^\Gamma := \widetilde{\Phi}_{j_0}^\Gamma$. For arbitrarily $s \geq 0$ let the Sobolev spaces $H^s_{\langle\cdot,\cdot\rangle}(\Gamma)$ be the closure of all *globally continuous*, patchwise C^∞-functions on Γ with respect to the norm

$$\|v\|_{H^s_{\langle\cdot,\cdot\rangle}(\Gamma)} := \sum_{i=1}^N \|v \circ \gamma_i\|_{H^s(\square)}.$$

The space $L^2_{\langle\cdot,\cdot\rangle}(\Gamma)$ indicates as usual the Sobolev space $H^0_{\langle\cdot,\cdot\rangle}(\Gamma)$. The Sobolev space $H^{-s}_{\langle\cdot,\cdot\rangle}(\Gamma)$, $s<0$, indicates the dual of $H^s_{\langle\cdot,\cdot\rangle}(\Gamma)$ with respect to the modified inner product (20), i.e.,

$$\|v\|_{H^{-s}_{\langle\cdot,\cdot\rangle}(\Gamma)} := \sup_{w\in H^s_{\langle\cdot,\cdot\rangle}(\Gamma)} \frac{\langle v,w\rangle}{\|w\|_{H^s_{\langle\cdot,\cdot\rangle}(\Gamma)}}.$$

Proposition 1.7. *The collection of wavelets Ψ^Γ and $\widetilde{\Psi}^\Gamma$ form biorthogonal Riesz bases in $L^2_{\langle\cdot,\cdot\rangle}(\Gamma)$. The primal wavelets satisfy the cancellation property* (23)*. Furthermore, there holds the norm equivalence*

$$\|v\|^2_{H^s_{\langle\cdot,\cdot\rangle}(\Gamma)} \sim \sum_{j\geq j_0-1}\sum_{\boldsymbol{\xi}\in\nabla^\Gamma_j} 2^{2sj}\big|\langle v,\widetilde{\psi}^\Gamma_{j,\boldsymbol{\xi}}\rangle\big|^2, \qquad s\in(-\widetilde{\gamma},\gamma),$$

$$\|v\|^2_{H^s_{\langle\cdot,\cdot\rangle}(\Gamma)} \sim \sum_{j\geq j_0-1}\sum_{\boldsymbol{\xi}\in\nabla^\Gamma_j} 2^{2sj}\big|\langle v,\psi^\Gamma_{j,\boldsymbol{\xi}}\rangle\big|^2, \qquad s\in(-\gamma,\widetilde{\gamma}),$$

with γ and $\widetilde{\gamma}$ denoting the regularity of the Cohen-Daubechies-Feauveau wavelets.

Unfortunately, the cancellation property is not satisfied with respect to the canonical inner product. Clearly, (24) is valid if both wavelets, $\psi^\Gamma_{j,\boldsymbol{\xi}}$ and $\psi^\Gamma_{j',\boldsymbol{\xi}'}$, are supported on a single patch. We mention that for wavelets supported on several patches this estimate remains true only if the fundamental tensor of differential geometry $\mathbf{K}_i$ is continuous across the interfaces of intersection patches.

According to [14], the Sobolev spaces $H^s(\Gamma)$ and $H^s_{\langle\cdot,\cdot\rangle}(\Gamma)$ are isomorphic in the range $s\in\big(-\frac{1}{2},\min\big\{\frac{3}{2},s_\Gamma\big\}\big)$, This yields the norm equivalences

$$\|v\|^2_{H^s(\Gamma)} \sim \sum_{j\geq j_0-1}\sum_{\boldsymbol{\xi}\in\nabla^\Gamma_j} 2^{2sj}\big|\big(v,\widetilde{\psi}^\Gamma_{j,\boldsymbol{\xi}}\big)_{L^2(\Gamma)}\big|^2, \qquad s\in\big(-\min\big\{\tfrac{1}{2},\widetilde{\gamma}\big\},\min\big\{\tfrac{3}{2},\gamma\big\}\big),$$

$$\|v\|^2_{H^s(\Gamma)} \sim \sum_{j\geq j_0-1}\sum_{\boldsymbol{\xi}\in\nabla^\Gamma_j} 2^{2sj}\big|\big(v,\psi^\Gamma_{j,\boldsymbol{\xi}}\big)_{L^2(\Gamma)}\big|^2, \qquad s\in\big(-\min\big\{\tfrac{1}{2},\gamma\big\},\min\big\{\tfrac{3}{2},\widetilde{\gamma}\big\}\big).$$

In particular, $s=0$ implies the Riesz property of the collections Ψ^Γ and $\widetilde{\Psi}^\Gamma$, respectively.

Algorithm 1 This algorithm computes the two scale decomposition $\widetilde{\Phi}_{j+1}^{\Gamma}\mathbf{a}^{(j+1)} = \widetilde{\Phi}_{j}^{\Gamma}\mathbf{a}^{(j)} + \widetilde{\Psi}_{j}^{\Gamma}\mathbf{b}^{(j)}$, where $\mathbf{a}^{(j)} = \left[a_{\boldsymbol{\xi}}^{(j)}\right]_{\boldsymbol{\xi}\in\Delta_j^{\Gamma}}$ and $\mathbf{b}^{(j)} = \left[b_{\boldsymbol{\xi}}^{(j)}\right]_{\boldsymbol{\xi}\in\nabla_j^{\Gamma}}$.

initialization: $\mathbf{a}^{(j)} := \mathbf{b}^{(j)} := \mathbf{0}$
for $i = 1$ **to** N **do begin**
  for all $\mathbf{k} \in \Delta_j^{\square}$ **do begin** C: compute coefficients of $\widetilde{\Phi}_j^{\Gamma}$
    for all $\mathbf{k}' \in \Delta_{j+1}^{\square}$ **do begin**
      $a_{\gamma_i(\mathbf{k})}^{(j)} = a_{\gamma_i(\mathbf{k})}^{(j)} + \left[\mathbf{M}_{j,0}^{\square}\right]_{\mathbf{k}',\mathbf{k}} a_{\gamma_i(\mathbf{k}')}^{(j+1)} / r\left(\gamma_i(\mathbf{k})\right)$
    end
  end
  for all $\mathbf{k} \in \nabla_j^{\square}$ **do begin** C: compute coefficients of $\widetilde{\Psi}_j^{\Gamma}$
    for all $\mathbf{k}' \in \Delta_{j+1}^{\square}$ **do begin**
      $b_{\gamma_i(\mathbf{k})}^{(j)} = b_{\gamma_i(\mathbf{k})}^{(j)} + \left[\mathbf{M}_{j,1}^{\square}\right]_{\mathbf{k}',\mathbf{k}} a_{\gamma_i(\mathbf{k}')}^{(j+1)} / r\left(\gamma_i(\mathbf{k})\right)$
    end
  end
end

Algorithm 2 This algorithm computes the two scale decomposition $\Phi_{j+1}^{\Gamma}\mathbf{a}^{(j+1)} = \Phi_j^{\Gamma}\mathbf{a}^{(j)} + \Psi_j^{\Gamma}\mathbf{b}^{(j)}$, where $\mathbf{a}^{(j)} = \left[a_{\boldsymbol{\xi}}^{(j)}\right]_{\boldsymbol{\xi}\in\Delta_j^{\Gamma}}$ and $\mathbf{b}^{(j)} = \left[b_{\boldsymbol{\xi}}^{(j)}\right]_{\boldsymbol{\xi}\in\nabla_j^{\Gamma}}$.

---

initialization: $\mathbf{a}^{(j)} := \mathbf{b}^{(j)} := \mathbf{0}$
for $i = 1$ **to** N **do begin**
  for all $\mathbf{k} \in \Delta_j^{\square}$ **do begin** C: compute coefficients of Φ_j^{Γ}
    for all $\mathbf{k}' \in \Delta_{j+1}^{\square}$ **do begin**
      $a_{\gamma_i(\mathbf{k})}^{(j)} = a_{\gamma_i(\mathbf{k})}^{(j)} + \left[\mathbf{M}_{j,0}^{\square}\right]_{\mathbf{k}',\mathbf{k}} a_{\gamma_i(\mathbf{k}')}^{(j+1)} / r\left(\gamma_i(\mathbf{k}')\right)$
    end
  end
  for all $\mathbf{k} \in \nabla_j^{\square}$ **do begin** C: compute coefficients of $\breve{\Psi}_j^{\Gamma}$
    for all $\mathbf{k}' \in \Delta_{j+1}^{\square}$ **do begin**
      $b_{\gamma_i(\mathbf{k})}^{(j)} = b_{\gamma_i(\mathbf{k})}^{(j)} + \left[\mathbf{M}_{j,1}^{\square}\right]_{\mathbf{k}',\mathbf{k}} a_{\gamma_i(\mathbf{k}')}^{(j+1)} / r\left(\gamma_i(\mathbf{k}')\right)$
    end
  end
end
for $i = 1$ **to** N **do begin**
  for all $\mathbf{k} \in \nabla_j^{\square}$ **do begin** C: add scaling functions to $\breve{\Psi}_j^{\Gamma}$
    for all $\mathbf{k}' \in \Delta_j^{\square}$ **do begin**
      $b_{\gamma_i(\mathbf{k})}^{(j)} = b_{\gamma_i(\mathbf{k})}^{(j)} - \left[\mathbf{L}_j^{\square}\right]_{\mathbf{k}',\mathbf{k}} a_{\gamma_i(\mathbf{k}')}^{(j)} / r\left(\gamma_i(\mathbf{k}')\right)$
    end
  end
end

---

2 The wavelet Galerkin scheme

This section presents a fully discrete wavelet Galerkin scheme for boundary integral equations. In the first subsection we discretize a given boundary integral equation. Then, in subsection 2.2 we introduce the a-priori matrix compression which reduces the relevant matrix coefficients to an asymptotically linear number. In subsections 2.3 and 2.4 we point out the computation of the compressed matrix. Next, in subsection 2.5 we introduce an a-posteriori compression which reduces again the number of matrix coefficients. The last subsection is dedicated to the preconditioning of system matrices which arise from boundary integral operators of nonzero order.

For the sake of simplicity, we skip the suffices Γ of the spaces and their bases. The collection $\Psi_J := \bigcup_{j\geq j_0-1}^{J-1}$ with a capital J denotes the wavelet basis of V_J. Moreover $N_J := |\Psi_J|$ indicates the number of unknowns on the level J.

2.1 Discretization

Generally written, a boundary integral equation for the unknown density $\rho \in H^q(\Gamma)$ is given by

$$\mathcal{A}\rho = f \quad \text{on } \Gamma. \tag{36}$$

Hereby, $\mathcal{A} : H^q(\Gamma) \to H^{-q}(\Gamma)$ denotes a boundary integral operator of the order $2q$ and $f \in H^{-q}(\Gamma)$ indicates the right hand side. Consequently, the variational formulation of (36) reads

$$\text{seek } \rho \in H^q(\Gamma) : \quad (\mathcal{A}\rho, \eta)_{L^2(\Gamma)} = (f, \eta)_{L^2(\Gamma)} \quad \forall\ \eta \in H^q(\Gamma). \tag{37}$$

It is well known, that the variational formulation (37) is equivalent to the boundary integral equation (36), see e.g. [18, 25] for details.

For the Galerkin scheme we replace the energy space $H^q(\Gamma)$ in the variational formulation (37) by the finite dimensional spaces V_J introduced in the previous section. Then, we arrive at the problem

$$\text{seek } \rho_J \in V_J : \quad (\mathcal{A}\rho_J, \eta_J)_{L^2(\Gamma)} = (f, \eta_J)_{L^2(\Gamma)} \quad \forall\ \eta_J \in V_J.$$

Equivalently, due to the finite dimension of V_J, the ansatz $\rho_J = \Psi_J \boldsymbol{\rho}_J$ together with

$$\mathbf{A}_J^\psi := \big(\mathcal{A}\Psi_J, \Psi_J\big)_{L^2(\Gamma)}, \qquad \mathbf{f}_J^\psi := \big(f, \Psi_J\big)_{L^2(\Gamma)},$$

yields the wavelet Galerkin scheme

$$\mathbf{A}_J^\psi \boldsymbol{\rho}_J^\psi = \mathbf{f}_J^\psi. \tag{38}$$

The system matrix $\mathbf{A}_J^\psi$ is quasi-sparse and might be compressed to $\mathcal{O}(N_J)$ nonzero matrix entries if the wavelets have a sufficiently large number of vanishing moments. The remainder of this paper is devoted to the efficient computation of the system matrix.

Remark 2.1. *Replacing the wavelet basis Ψ_J by the single-scale basis Φ_J yields the traditional single-scale Galerkin scheme*

$$\mathbf{A}_J^\phi \boldsymbol{\rho}_J^\phi = \mathbf{f}_J^\phi,$$

where $\mathbf{A}_J^\phi := \big(\mathcal{A}\Phi_J, \Phi_J\big)_{L^2(\Gamma)}$, $\mathbf{f}_J^\phi := \big(f, \Phi_J\big)_{L^2(\Gamma)}$ *and* $\rho_J = \Phi_J \boldsymbol{\rho}_J$. *This scheme is related to the wavelet Galerkin scheme by*

$$\mathbf{A}_J^\psi = \mathbf{T}_J \mathbf{A}_J^\phi \mathbf{T}_J^T, \qquad \boldsymbol{\mu}_J^\psi = \mathbf{T}_J^{-T} \boldsymbol{\mu}_J^\phi, \qquad \mathbf{f}_J^\psi = \mathbf{T}_J \mathbf{f}_J^\phi,$$

where $\mathbf{T}_J$ *denotes the wavelet transform. The system matrix* $\mathbf{A}_J^\phi$ *is densely populated. Therefore, the costs of solving a given boundary integral equation traditionally in the single-scale basis is at least* $\mathcal{O}(N_J^2)$.

2.2 A-priori compression

The discretization of a boundary integral operator $\mathcal{A} : H^q(\Gamma) \to H^{-q}(\Gamma)$ by wavelets with a sufficiently large number of vanishing moments (22) or a corresponding cancellation property (23) yields quasi-sparse matrices. In a first compression step all matrix entries, for which the distances of the supports of the corresponding ansatz and test functions are bigger than a level depending cut-off parameter $\mathcal{B}_{j,j'}$, are set to zero. In the second compression step also some of those matrix entries are neglected, for which the corresponding ansatz and test functions have overlapping supports.

First, we introduce the abbreviation

$$\begin{aligned} \Theta_{j,\mathbf{k}} &:= \operatorname{conv}\operatorname{hull}(\operatorname{supp}\psi_{j,\mathbf{k}}), \\ \Xi_{j,\mathbf{k}} &:= \operatorname{sing}\operatorname{supp}\psi_{j,\mathbf{k}}. \end{aligned}$$

Note that $\Theta_{j,\mathbf{k}}$ denotes the convex hull to the support of $\psi_{j,\mathbf{k}}$ while $\Xi_{j,\mathbf{k}}$ denotes the so-called *singular support* of $\psi_{j,\mathbf{k}}$, i.e., those points where $\psi_{j,\mathbf{k}}$ is not smooth.

The compressed system matrix $\mathbf{A}_J^\psi$ corresponding to the boundary integral operator $\mathcal{A}$ is defined by

$$[\mathbf{A}_J^\psi]_{(j,\mathbf{k}),(j',\mathbf{k}')} := \begin{cases} 0, & \operatorname{dist}\big(\Theta_{j,\mathbf{k}}, \Theta_{j',\mathbf{k}'}\big) > \mathcal{B}_{j,j'},\ j, j' \geq j_0, \\ 0, & \operatorname{dist}\big(\Xi_{j,\mathbf{k}}, \Theta_{j',\mathbf{k}'}\big) > \mathcal{B}'_{j,j'},\ j' > j, \\ 0, & \operatorname{dist}\big(\Theta_{j,\mathbf{k}}, \Xi_{j',\mathbf{k}'}\big) > \mathcal{B}'_{j,j'},\ j > j', \\ \big(\mathcal{A}\psi_{j',\mathbf{k}'}, \psi_{j,\mathbf{k}}\big)_{L^2(\Gamma)}, & \text{otherwise.} \end{cases} \tag{39}$$

Herein, choosing

$$a, a' > 1, \qquad d < \delta, \delta' < \widetilde{d} + 2q, \tag{40}$$

the cut-off parameters $\mathcal{B}_{j,j'}$ and $\mathcal{B}'_{j,j'}$ are set as follows

$$\begin{aligned}\mathcal{B}_{j,j'} &= a \ \max\left\{2^{-\min\{j,j'\}}, 2^{\frac{2J(\delta-q)-(j+j')(\delta+\tilde{d})}{2(\tilde{d}+q)}}\right\},\\ \mathcal{B}'_{j,j'} &= a' \max\left\{2^{-\max\{j,j'\}}, 2^{\frac{2J(\delta'-q)-(j+j')\delta'-\max\{j,j'\}\tilde{d}}{\tilde{d}+2q}}\right\}.\end{aligned} \tag{41}$$

The resulting structure of the compressed matrix is figuratively called *finger structure*, cf. figure 5. It is shown in [30] that this compression strategy does not compromise the stability and accuracy of the underlying Galerkin scheme.

Theorem 2.2. *Let the system matrix* $\mathbf{A}_J^\psi$ *be compressed in accordance with* (39), (40) *and* (41). *Then, the wavelet Galerkin scheme is stable and the error estimate*

$$\|\rho - \rho_J\|_{H^{2q-d}(\Gamma)} \lesssim 2^{-2J(d-q)} \|\rho\|_{H^d(\Gamma)} \tag{42}$$

holds, where $\rho \in H^d(\Gamma)$ *denotes the exact solution of the given boundary integral equation* $\mathcal{A}\rho = f$ *and* $\rho_J = \Psi_J \boldsymbol{\rho}_J^\psi$ *is the numerically computed solution, i.e.,* $\widetilde{\mathbf{A}}_J^\psi \boldsymbol{\rho}_J^\psi = \mathbf{f}^\psi$. *Consequently, we obtain the optimal order of convergence of the Galerkin scheme.*

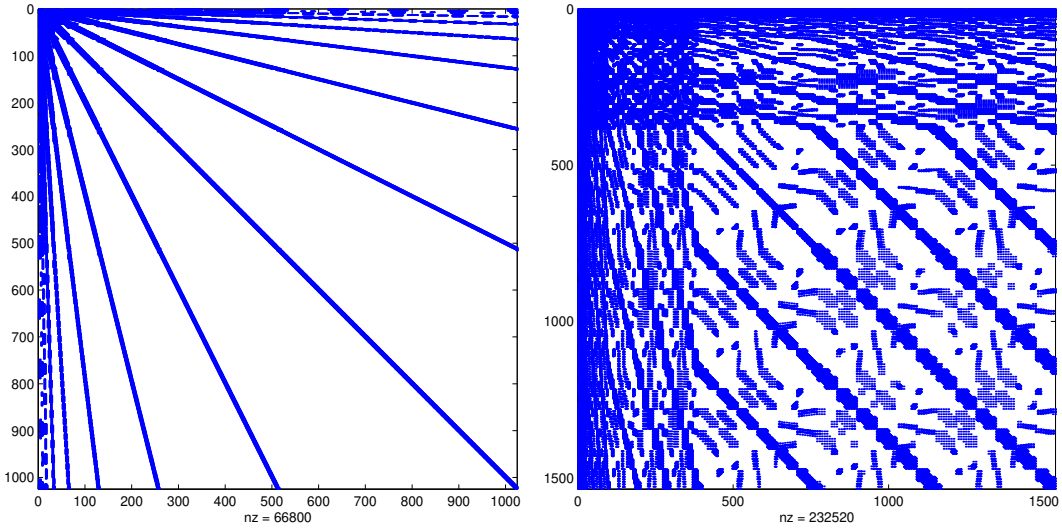

Figure 5: The finger structure of the compressed system matrix computed with respect to the two dimensional (left) and the three dimensional (right) unit spheres.

The next theorem shows that the over-all complexity of assembling the compressed system matrix is $\mathcal{O}(N_J)$ even if each entry is weighted by a logarithmical penalty term [21]. We mention that the choice $\alpha = 0$ proves that the a-priori compression yields a system matrix with only $\mathcal{O}(N_J)$ nonzero matrix entries.

Theorem 2.3. *Let the system matrix* $\mathbf{A}_J^{\psi} = (\mathcal{A}\Psi_J, \Psi_J)_{L^2(\Gamma)}$ *be compressed according to* (39). *The complexity of computing this compressed matrix is* $\mathcal{O}(N_J)$ *if the calculation of its entries* $(\mathcal{A}\psi_{j',\mathbf{k}'}, \psi_{j,\mathbf{k}})_{L^2(\Gamma)}$ *is performed in* $\mathcal{O}\big(\big[J-\frac{j+j'}{2}\big]^{\alpha}\big)$ *operations with some* $\alpha \geq 0$.

2.3 Setting up the compression pattern

In order to compute the matrix compression we cannot check the distance criterion 39 for each matrix coefficient since this leads to $\mathcal{O}(N_J^2)$ functions calls. The way out is to exploit the underlying tree structure with respect to the supports of the wavelets. We call a wavelet $\psi_{j+1,\text{son}}$ a son of $\psi_{j,\text{father}}$ if $\Theta_{j+1,\text{son}} \subseteq \Theta_{j,\text{father}}$.

Lemma 2.4. *We consider* $\Theta_{j+1,\text{son}} \subseteq \Theta_{j,\text{father}}$ *and* $\Theta_{j'+1,\text{son}} \subseteq \Theta_{j',\text{father}}$.

1. *If*

$$\operatorname{dist}\left(\Theta_{j,\text{father}}, \Theta_{j',\text{father}'}\right) > \mathcal{B}_{j,j'}$$

then there holds

$$\begin{aligned}\operatorname{dist}\left(\Theta_{j+1,\text{son}}, \Theta_{j',\text{father}'}\right) &> \mathcal{B}_{j+1,j'}\\ \operatorname{dist}\left(\Theta_{j+1,\text{son}}, \Theta_{j'+1,\text{son}'}\right) &> \mathcal{B}_{j+1,j+1'}.\end{aligned}$$

2. *For* $j > j'$ *suppose*

$$\operatorname{dist}\left(\Theta_{j,\text{father}}, \Xi_{j',\text{father}'}\right) > \mathcal{B}'_{j,j'}$$

then we can conclude that

$$\operatorname{dist}\left(\Theta_{j+1,\text{son}}, \Xi_{j',\text{father}'}\right) > \mathcal{B}'_{j+1,j'}$$

With the help of this lemma we have to check the distance criteria only for coefficients which stem from subdivision of calculated coefficients on a coarser level. Therefore, the resulting procedure of checking the distance criteria is still linear.

2.4 Assembly of the compressed matrix

Up to this point we know that the compressed system matrix has at most $\mathcal{O}(N_J)$ nonzero entries. Now we discuss how to compute the relevant matrix coefficients $(\mathcal{A}\psi_{j',\mathbf{k}'}, \psi_{j,\mathbf{k}})_{L^2(\Gamma)}$ in the Galerkin approach. The matrix entries are given by a double integral over the support of the basis functions, which in the case of a three-dimensional problem is a doubled two-dimensional integration. Unfortunately even for cardinal B-splines it is not possible to determine the matrix entries analytically.

Therefore we are forced to compute the matrix coefficients by quadrature rules. This causes an additional error which has to be controlled and it takes place against a background of realizing asymptotically optimal accuracy while preserving efficiency. This means the numerical methods have to be chosen carefully such that the desired linear complexity of the algorithm is not violated. However, it is not obvious that the complexity in order to compute the relevant coefficients is still linear. It is an immediate consequence of the fact that we require only a level dependent precision of quadrature, cf. [21, 30].

Lemma 2.5. *Let the error of quadrature for computing the relevant matrix coefficients* $(\mathcal{A}\psi_{j',\mathbf{k}'}, \psi_{j,\mathbf{k}})_{L^2(\Gamma)}$ *be bounded by the level dependent accuracy*

$$\varepsilon_{j,j'} \sim \min\left\{2^{-|j-j'|}, 2^{-2(J-\frac{j+j'}{2})\frac{\delta-q}{d+q}}\right\} 2^{2Jq} 2^{-2d'(J-\frac{j+j'}{2})} \tag{43}$$

with some $d' > d$ *and* $\delta \in (d, \widetilde{d}+r)$ *from* (40)*. Then, the Galerkin scheme is stable and converges with the optimal order* (42)*.*

From (43) we conclude that the entries on the coarse grids have to be computed with the full accuracy while the entries on the finer grids are allowed to have less accuracy. Unfortunately, the domains of integration are very large on coarser scales.

According to the fact that a wavelet is a linear combination of scaling functions the numerical integration can be reduced to interactions of polynomial form functions on certain elements. This suggests to employ an element-based representation of the wavelets like illustrated in figure 6 in the case of a piecewise linear wavelet. Consequently, we have only to deal with integrals of the form

$$I(\Gamma_{i,j,k}, \Gamma_{i',j',k'}) := \int_{\Gamma_{i,j,k}} \int_{\Gamma_{i',j',k'}} k(\mathbf{x},\mathbf{y}) p_l\big(\gamma_i^{-1}(\mathbf{x})\big) p_{l'}\left(\gamma_{i'}^{-1}(\mathbf{y})\right)\, d\sigma_{\mathbf{y}}\, d\sigma_{\mathbf{x}} \tag{44}$$

with p_l denoting the polynomial form functions. This is quite similar to the traditional Galerkin discretization. The main difference is that in the wavelet approach the elements may appear on different levels due to the multilevel hierarchy of wavelet bases.

Difficulties arise if the domains of integration are very close together relatively to their size. We have to apply numerical integration carefully in order to keep the number of evaluations of the kernel function at the quadrature knots moderate and to fulfill the assumptions of theorem 2.3. In [21, 30] a geometrically graded subdivision is proposed in combination with varying polynomial degrees of approximation in the integration rules, cf. figure 7. It is shown in [21] that the combination of tensor product Gauß-Legendre quadrature rules with such a *hp*-quadrature scheme leads to the number of quadrature points satisfying the assumption of theorem 2.3 with $\alpha = 4$.

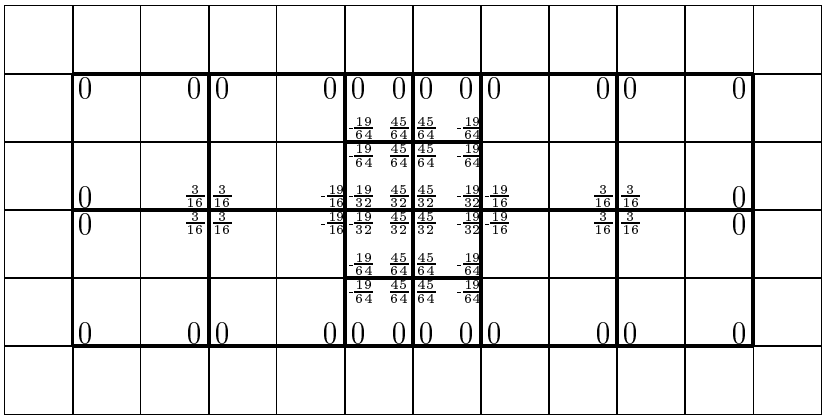

Figure 6: The element-based representation of a piecewise linear wavelet with four vanishing moments.

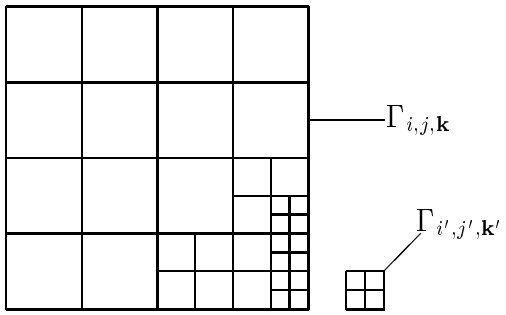

Figure 7: Adaptive subdivision of the domains of integration.

Since the kernel function has a singularity on the diagonal we are confronted with singular integrals if the domains of integration live on the same level and have any points in common. This situation appears if the underlying elements are identical or share a common edge or vertex. Such singular integrals can be treated by the so-called *Duffy-trick* [16, 29], which transform the singular integrands onto analytical ones.

2.5 A-posteriori compression

Let $\mathcal{A} : H^{-q}(\Gamma) \to H^q(\Gamma)$ be a boundary integral operator and $\mathbf{A}_J^\psi$ the associated system matrix compressed according to subsection 2.2. If the entries of the compressed system matrix $\mathbf{A}_J^\psi$ have been computed, we may apply an a-posteriori compression by setting all entries to zero, which are smaller than a level depending threshold. That way, a matrix $\widetilde{\mathbf{A}}_J^\psi$ is obtained which has less nonzero entries than the matrix $\mathbf{A}_J^\psi$. Clearly, this does not accelerate the calculation of the matrix

coefficients. But the requirement to the memory is reduced if the system matrix has to be stored. For instance, this is advantageous for the coupling of FEM and BEM, cf. [22, 23]. To our experiences this procedure reduces the number of nonzero coefficients by a factor 2–5.

Theorem 2.6. *We define the a-posteriori compression by*

$$\left[\widetilde{\mathbf{A}}^{\psi}\right]_{(j,\mathbf{k}),(j',\mathbf{k}')} = \begin{cases} 0, & \text{if } \left|\left[\mathbf{A}^{\psi}\right]_{(j,\mathbf{k}),(j',\mathbf{k}')}\right| \le \varepsilon_{j,j'}, \\ \left[\mathbf{A}^{\psi}\right]_{(j,\mathbf{k}),(j',\mathbf{k}')}, & \text{if } \left|\left[\mathbf{A}^{\psi}\right]_{(j,\mathbf{k}),(j',\mathbf{k}')}\right| > \varepsilon_{j,j'}. \end{cases}$$

Herein, the level dependent threshold $\varepsilon_{j,j'}$ is chosen as in (43) with some $d' > d$ and $\delta \in (d, \widetilde{d} + r)$ from (40). Then, the optimal order of convergence of the Galerkin scheme is achieved.

2.6 Wavelet preconditioning

Let $\mathcal{A} : H^q(\Gamma) \to H^{-q}(\Gamma)$ denote a boundary integral operator of the order $2q$ with $q \neq 0$. Then, the corresponding system matrix $\mathbf{A}_J^{\psi}$ is ill conditioned. In fact, there holds $\mathrm{cond}_{l^2} \mathbf{A}_J^{\psi} \sim 2^{2J|q|}$. According to [6, 30], the wavelet approach offers a simple diagonal preconditioner based on the norm equivalences.

Theorem 2.7. *Let the diagonal matrix $\mathbf{D}_J^r$ defined by*

$$\left[\mathbf{D}_J^r\right]_{(j,k),(j',k')} = 2^{rj}\delta_{j,j'}\delta_{k,k'}, \quad k \in \nabla_j, \quad k' \in \nabla_{j'}, \quad j_0 - 1 \le j, j' < J. \tag{45}$$

Then, if $\mathcal{A} : H^q(\Gamma) \to H^{-q}(\Gamma)$ denotes a boundary integral operator of the order $2q$ with $\widetilde{\gamma} > -q$, the diagonal matrix $\mathbf{D}_J^{2q}$ defines a preconditioner to $\mathbf{A}_J^{\psi}$, i.e.,

$$\mathrm{cond}_{l^2}(\mathbf{D}_J^{-q}\mathbf{A}_J^{\psi}\mathbf{D}_J^{-q}) \sim 1.$$

Remark 2.8. *The coefficients on the main diagonal of $\mathbf{A}_J^{\psi}$ satisfy $\left(\mathcal{A}\psi_{j,\mathbf{k}}, \psi_{j,\mathbf{k}}\right)_{L^2(\Gamma)} \sim 2^{2qj}$. Therefore, the above preconditioning can be replaced by a diagonal scaling. In fact, the diagonal scaling improves and simplifies the wavelet preconditioning.*

As the numerical results in [24] confirm, this preconditioning works well in the two dimensional case. However, in the three dimensions, the results are not satisfactory, cf. 8. In spite of the wavelet preconditioning, the condition numbers with respect to the wavelets are not significantly better than with respect to the single-scale basis. We mention that the situation becomes even worse for operators defined on more complicated manifolds.

A slight modification of the wavelet preconditioner yields much better results. The simple trick is to combine the above preconditioner with the mass matrix which yields an appropriate operator based preconditioning.

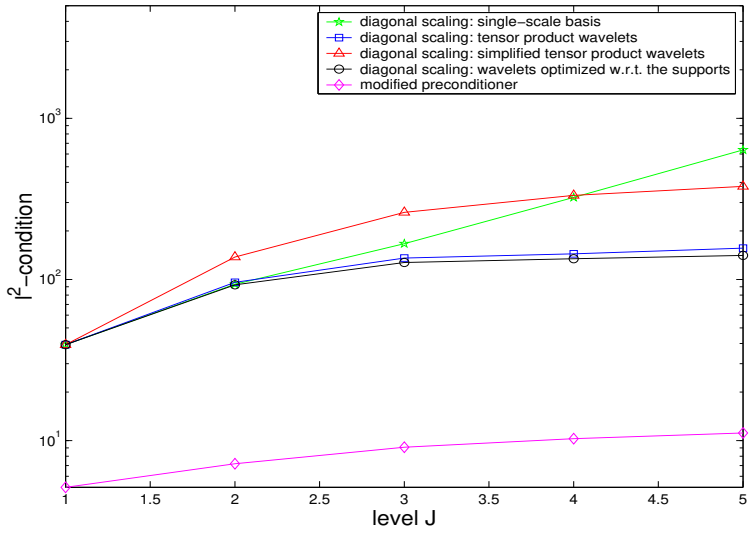

Figure 8: The l^2-condition numbers with respect to the single layer operator on the unit square and piecewise linear wavelets with four vanishing moments.

Theorem 2.9. *We consider a boundary integral operator* $\mathcal{A} : H^q(\Gamma) \to H^{-q}(\Gamma)$ *with corresponding Galerkin matrix* $\mathbf{A}_J^\psi$. *Let* $\mathbf{D}_J^r$ *be defined as in* (45) *and let* $\mathbf{B}_J^\psi := (\Psi_J, \Psi_J)_{L^2(\Gamma)}$ *denote the mass matrix. Then, if* $\widetilde{\gamma} > -q$, *the matrix* $\mathbf{C}_J^{2q} = \mathbf{D}_J^q \mathbf{B}_J^\psi \mathbf{D}_J^q$ *defines a preconditioner to* $\mathbf{A}_J^\psi$, *i.e.,*

$$\mathrm{cond}_{l^2}\left(\left(\mathbf{C}_J^{2q}\right)^{-1/2} \mathbf{A}_J^\psi \left(\mathbf{C}_J^{2q}\right)^{-1/2}\right) \sim 1.$$

One figures out of figure 8 that this preconditioner decreases the condition numbers impressively. Let us remark that the condition depends only on the underlying spaces and not on the chosen wavelet basis. To our experiences the condition reduces about the factor 10–100 compared to the preconditioner (45).

3 Numerical Results

This section is dedicated to numerical examples in order to confirm our theory. Firstly, we compute a Dirichlet problem. We use the indirect formulation for the double layer operator which gives a Fredholm's integral equation of the second kind. This is approximated by using piecewise constant wavelets. Secondly, we solve a Neumann problem employing the indirect formulation for the hypersingular operator. The discretization requires globally continuous piecewise linear wavelets. We mention that both problems are chosen such that the solutions are known analytically in order to measure the error of method.

3.1 Dirichlet Problem

For a given $f \in H^{1/2}(\Gamma)$ we consider an interior Dirichlet problem, i.e., we seek $u \in H^1(\Omega)$ such that

$$\begin{aligned} \Delta u &= 0 \qquad \text{in } \Omega, \\ u &= f \qquad \text{on } \Gamma. \end{aligned} \tag{46}$$

The domain Ω is described by the set difference of the cube $[-1,1]^3$ and three cylinders with radii 0.5, cf. figure 9. The boundary Γ is parametrized via 48 patches. Choosing the harmonical function

$$u(\mathbf{x}) = 4x^2 - 3y^2 - z^2$$

and setting $f := u|_\Gamma$ the problem (46) has the unique solution u.

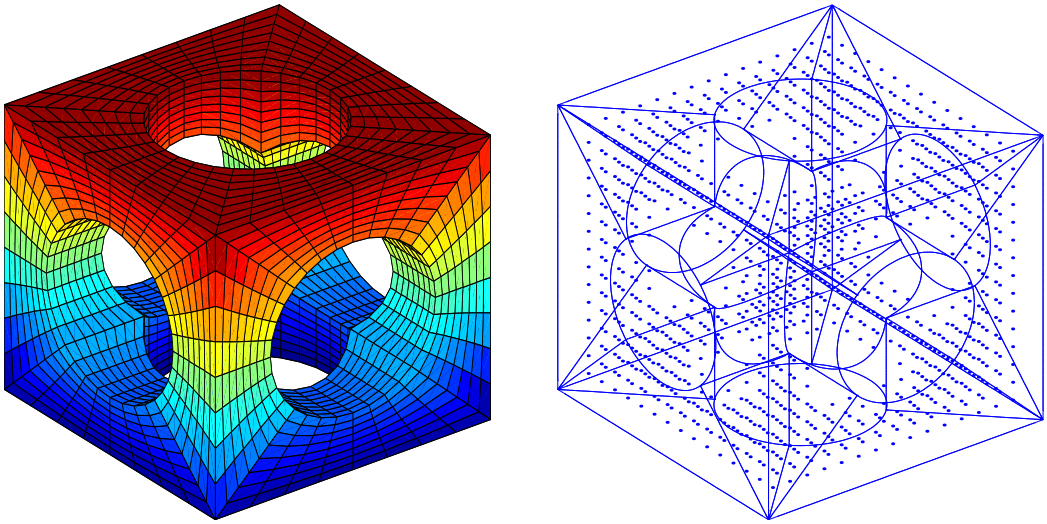

Figure 9: The mesh on the surface Γ and the evaluation points $\mathbf{x}_i$ of the potential.

Employing the double layer operator

$$(\mathcal{K}\rho)(\mathbf{x}) := \int_\Gamma \frac{\partial}{\partial \mathbf{n}_\mathbf{y}} \frac{1}{\|\mathbf{x}-\mathbf{y}\|^2} \rho(\mathbf{y}) d\sigma_\mathbf{y}, \quad \mathbf{x} \in \Gamma, \tag{47}$$

yields the Fredholm integral equation of the second kind

$$\left(\mathcal{K} - \tfrac{1}{2} I\right)\rho = f \quad \text{on } \Gamma.$$

Herein, the operator on the left hand side defines an operator of the order 0. We discretize this equation by piecewise constant wavelets with three vanishing moments

which is in accordance with (40). In order to compare the different constructions from subsection 1.3 we compute the solution with respect to all wavelet bases shown in figure 1.

The density ρ given by the boundary integral equation (47) yields the solution u of the Dirichlet problem by application of the double layer operator

$$u = \mathcal{K}\rho \quad \text{in } \Omega. \tag{48}$$

We denote the discrete counterparts by

$$\mathbf{u} := [u(\mathbf{x}_i)], \quad \mathbf{u}_J^\phi := [(\mathcal{K}\rho_J^\phi)(\mathbf{x}_i)], \quad \mathbf{u}_J^\psi := [(\mathcal{K}\rho_J^\psi)(\mathbf{x}_i)], \tag{49}$$

where the evaluation points $\mathbf{x}_i$ are specified in figure 9. Herein, $\mathbf{u}_J^\phi$ indicates the approximation computed by the traditional Galerkin scheme while $\mathbf{u}_J^\psi$ stands for the numerical solution of the wavelet Galerkin scheme.

First, in table 1 we list the maximum norm of the absolute errors of $\mathbf{u}_J^\phi$ and $\mathbf{u}_J^\psi$. The latter one is tabulated only with respect to $\psi^{(1,3)}_{\text{optimized}}$ since the other wavelet bases yield nearly identical results. The columns titled by "contr." (contraction) contain the ratio of the absolute error obtained on the previous level divided by the present absolute error. The optimal order of convergence is quadratic which implies a contraction close to 4. As the results in table 1 confirm, the precisions of the single-scale and the compressed wavelet Galerkin scheme are rather similar.

unknowns		scaling functions $\phi^{(1)}$		wavelets $\psi^{(1,3)}_{\text{tensor}}$	
J	N_J	$\|\mathbf{u}-\mathbf{u}_J^\phi\|_\infty$	contr.	$\|\mathbf{u}-\mathbf{u}_J^\psi\|_\infty$	contr.
1	192	1.9	—	2.6	—
2	768	3.3e-1	4.0	4.1e-1	6.2
3	3072	5.7e-2	4.4	6.6e-2	6.2
4	12288	(1.4e-2)	(4.0)	1.3e-2	5.0
5	49152	(3.6e-3)	(4.0)	3.3e-3	4.0

Table 1: The maximum norm of the absolute errors of the discrete potential.

Figure 10 is concerned with the behaviour of the compression. We measure the compression rates by the ratio (in %) of the number of nonzero matrix coefficients and N_J^2. The left plot visualizes the a-priori compression and the right one the a-posteriori compression. The best compression rates are achieved with respect to the wavelets $\psi^{(1,3)}_{\text{optimized}}$. which issues from their small supports. For 49152 unknows only 0.78% of the matrix coefficients are relevant. After the a-posteriori compression this number is even reduced to 0.15%.

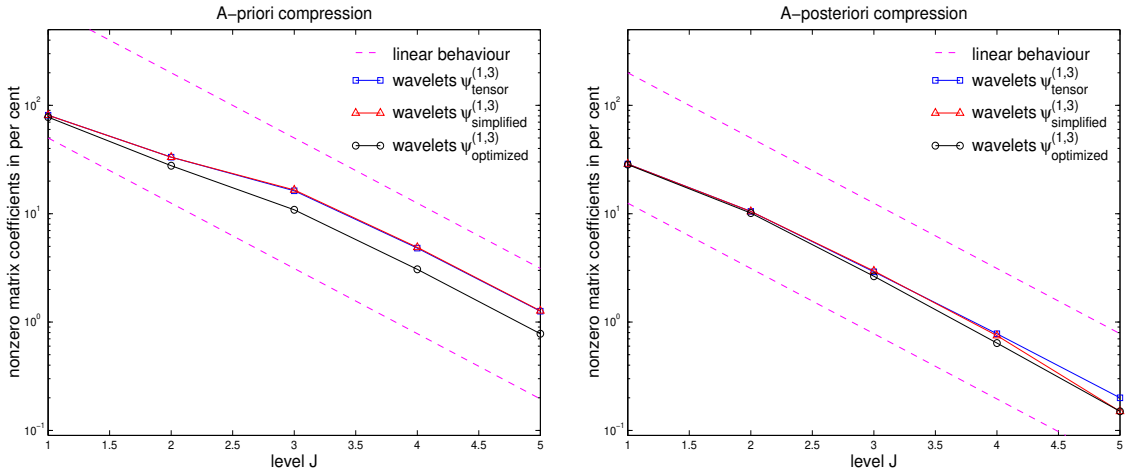

Figure 10: The compression rates of the a-priori and a-posteriori compression.

On figures out of table 2 the times required for computing and solving the linear equation system resulting from the Galerkin scheme. The best performance its achieved by the wavelet Galerkin scheme based on $\psi^{(1,3)}_{\text{optimized}}$. For $N_J = 49152$ we obtain the speed-up factor 11.4 in comparison with the single-scale scheme.

unknowns		computing times in seconds			
J	N_J	$\phi^{(1)}$	$\psi^{(1,3)}_{\text{tensor}}$	$\psi^{(1,3)}_{\text{simplified}}$	$\psi^{(1,3)}_{\text{optimized}}$
1	192	0.6	1.3	1.3	1.2
2	768	27	16	16	15
3	3072	473	292	236	191
4	12288	(7576)	2032	1522	1246
5	49152	(121216)	16345	11675	10597

Table 2: Comparison of the over-all computing times.

3.2 Neumann Problem

For a given $g \in H^{-1/2}(\Gamma)$ with $\int_\Gamma g(\mathbf{x})d\sigma = 0$ we treat a Neumann problem on the domain Ω, that is, we seek $u \in H^1(\Omega)$ such that

$$\begin{aligned} \Delta u &= 0 \qquad \text{in } \Omega, \\ \tfrac{\partial u}{\partial \mathbf{n}} &= g \qquad \text{on } \Gamma. \end{aligned} \tag{50}$$

The considered domain Ω is described as the union of two spheres $B_1([0,0,\pm 2]^T)$ and one connecting cylinder with the radius 0.5, compare figure 11. The boundary

Γ is represented via 14 patches. Choosing the harmonical function

$$u(\mathbf{x}) = \frac{(\mathbf{a}, \mathbf{x}-\mathbf{b})}{\|\mathbf{x}-\mathbf{b}\|^3}, \quad \mathbf{a} = [1,2,4]^T, \quad \mathbf{b} = [1,0,0]^T. \tag{51}$$

and setting $g := \frac{\partial u|_\Gamma}{\partial \mathbf{n}}$ the Neumann problem has the solution u modulo a constant.

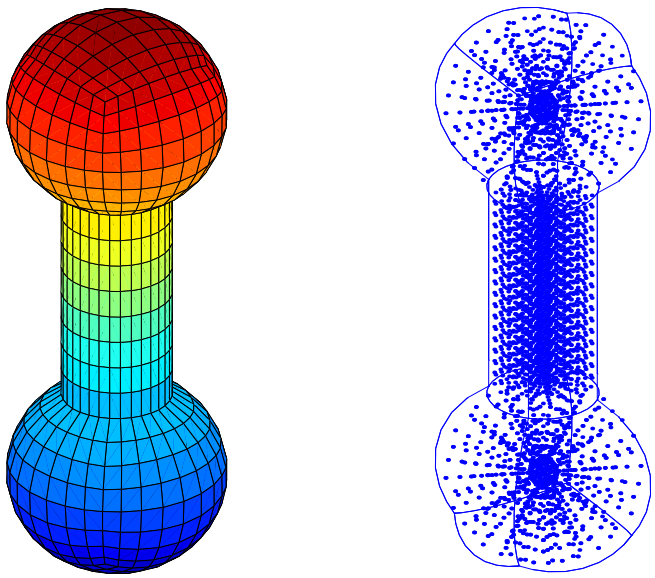

Figure 11: The mesh on the surface Γ and the evaluation points $\mathbf{x}_i$ of the potential.

The *hypersingular operator* $\mathcal{W}$ is given by

$$\mathcal{W}\rho(\mathbf{x}) := -\frac{1}{4\pi}\frac{\partial}{\partial \mathbf{n}_\mathbf{x}} \int_\Gamma \frac{\partial}{\partial \mathbf{n}_\mathbf{y}} \frac{1}{\|\mathbf{x}-\mathbf{y}\|^2} \rho(\mathbf{y}) d\sigma_\mathbf{y}, \quad \mathbf{x} \in \Gamma,$$

and defines an operator of order $+1$. In order to solve problem (50) we seek the density ρ satisfying the Fredholm integral equation of the first kind

$$\mathcal{W}\rho = g \quad \text{on } \Gamma. \tag{52}$$

Since $\mathcal{W}$ is symmetric and positive semidefinite, cf. [18, 25], one restricts ρ by the constraint $\int_\Gamma \rho(\mathbf{x}) d\sigma = 0$. We emphasize that the discretization of the hypersingular operator requires *globally continuous* piecewise linear wavelets. According to (40) piecewise linear wavelets have to provide two vanishing moments.

The density ρ given by the boundary integral equation (52) leads to the solution u of the Neumann problem by application of the double layer operator according to (48). The discrete counterparts are denoted as in (49), where the evaluation points $\mathbf{x}_i$ are specified in figure 11.

First, we compare the errors of approximation with respect to the discrete potentials. The order of convergence is cubic if the density is sufficiently smooth. Hence, the contraction should be close to 8. The results in table 3 suggest even a higher rate of convergence. The wavelet Galerkin scheme achieves the same accuracy as the traditional Galerkin scheme.

unknowns		scaling functions		wavelets	
J	N_J	$\|\mathbf{u}_J - \mathbf{u}_J^{\phi}\|_\infty$	contr.	$\|\mathbf{u}_J - \mathbf{u}_J^{\psi}\|_\infty$	contr.
1	58	7.1	—	7.6	—
2	226	4.3	1.4	4.2	1.8
3	898	1.2	3.6	1.2	3.5
4	3586	1.9e-1	6.3	1.9e-1	6.2
5	14338	(2.4e-2)	(8.0)	1.4e-2	14
6	57346	(3.0e-3)	(8.0)	4.8e-4	30

Table 3: The maximum norm of the absolute errors of the discrete potential.

The plots in figure 12 visualize the compression rates and computing times. On the left hand side we plot the number of nonzero coefficients in percent. For 57346 unknowns the matrix compression yields only 1.37 % and 0.73 % relevant matrix entries after a-priori and a-posteriori compression, respectively. On the right hand side one figures out the over-all computing times of the traditional discretization compared with those of the fast wavelet discretization. Note that we extrapolated the computing times of the traditional scheme to the levels 5 and 6. On level 6 the speed-up of the wavelet Galerkin scheme is about the factor 11 compared to the traditional scheme.

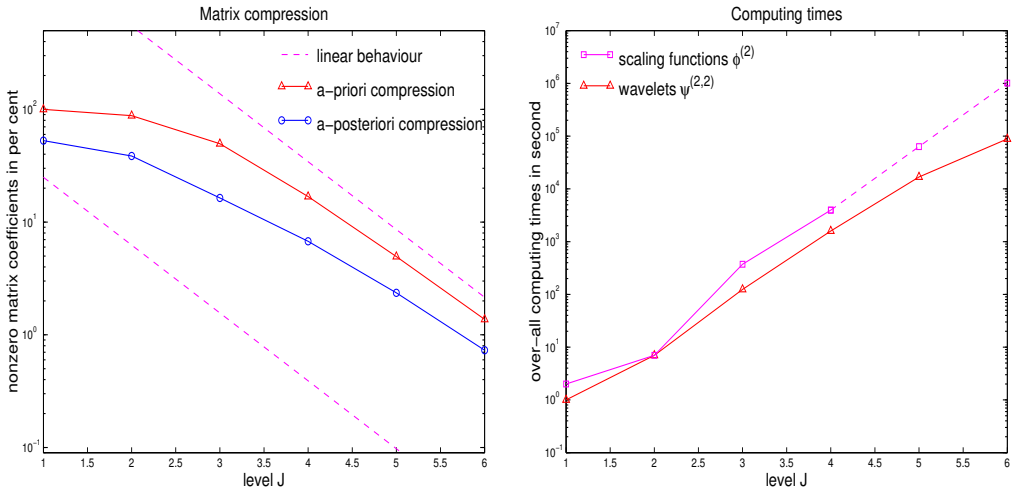

Figure 12: The compression rates and computing times.

References

[1] G. Beylkin, R. Coifman, and V. Rokhlin. The fast wavelet transform and numerical algorithms. *Comm. Pure and Appl. Math.*, 44:141–183, 1991.

[2] C. Canuto, A. Tabacco, and K. Urban. The wavelet element method, part I: Construction and analysis. *Appl. Comput. Harm. Anal.*, 6:1–52, 1999.

[3] J. Carnicer, W. Dahmen, and J. Peña. Local decompositions of refinable spaces. *Appl. Comp. Harm. Anal.*, 3:127–153, 1996.

[4] A. Cohen, I. Daubechies, and J.-C. Feauveau. Biorthogonal bases of compactly supported wavelets. *Pure Appl. Math.*, 45:485–560, 1992.

[5] A. Cohen and R. Masson. Wavelet adaptive method for second order elliptic problems – boundary conditions and domain decompsition. *Numer. Math.*, 86:193–238, 2000.

[6] W. Dahmen. Wavelet and multiscale methods for operator equations. *Acta Numerica*, 6:55–228, 1997.

[7] W. Dahmen, B. Kleemann, S. Prößdorf, and R. Schneider. A multiscale method for the double layer potential equation on a polyhedron. In H.P. Dikshit and C.A. Micchelli, editors, *Advances in Computational Mathematics*, pages 15–57, World Scientific Publ., Singapore, 1994.

[8] W. Dahmen, A. Kunoth, and K. Urban. Biorthogonal spline-wavelets on the interval – stability and moment conditions. *Appl. Comp. Harm. Anal.*, 6:259–302, 1999.

[9] W. Dahmen, S. Prößdorf, and R. Schneider. Multiscale methods for pseudodifferential equations. In L.L. Schumaker and G. Webb, editors, *Wavelet Analysis and its Applications*, volume 3, pages 191–235, 1993.

[10] W. Dahmen, S. Prößdorf, and R. Schneider. Wavelet approximation methods for periodic pseudodifferential equations. Part II – Fast solution and matrix compression. *Advances in Computational Mathematics*, 1:259–335, 1993.

[11] W. Dahmen, S. Prößdorf, and R. Schneider. Wavelet approximation methods for periodic pseudodifferential equations. Part I – Convergence analysis. *Mathematische Zeitschrift*, 215:583–620, 1994.

[12] W. Dahmen, S. Prößdorf, and R. Schneider. Multiscale methods for pseudodifferential equations on smooth manifolds. In C.K. Chui, L. Montefusco, and L. Puccio, editors, *Proceedings of the International Conference on Wavelets: Theory, Algorithms, and Applications*, pages 385–424, 1995.

[13] W. Dahmen and R. Schneider. Wavelets on manifolds II: Application to boundary element methods and pseudodifferential equations, 1996. Manuscript.

[14] W. Dahmen and R. Schneider. Composite wavelet bases for operator equations. *Math. Comp.*, 68:1533–1567, 1999.

[15] W. Dahmen and R. Schneider. Wavelets on manifolds I. Construction and domain decomposition. *Math. Anal.*, 31:184–230, 1999.

[16] M. Duffy. Quadrature over a pyramid or cube of integrands with a singularity at the vertex. *SIAM J. Numer. Anal.*, 19:1260–1262, 1982.

[17] L. Greengard and V. Rokhlin. A fast algorithm for particle simulation. *J. Comput. Phys.*, 73:325–348, 1987.

[18] W. Hackbusch. *Integralgleichungen.* B.G. Teubner, Stuttgart, 1989.

[19] W. Hackbusch. A sparse matrix arithmetic based on $\mathcal{H}$-matrices. Part I: Introduction to $\mathcal{H}$-matrices. *Computing*, 64:89–108, 1999.

[20] W. Hackbusch and Z.P. Nowak. On the fast matrix multiplication in the boundary element method by panel clustering. *Numer. Math.*, 54:463–491, 1989.

[21] H. Harbrecht. Wavelet Galerkin schemes for the boundary element method in three dimensions. *PHD Thesis, Technische Universität Chemnitz, Germany*, 2001.

[22] H. Harbrecht, F. Paiva, C. Pérez, and R. Schneider. Biorthogonal wavelet approximation for the coupling of FEM-BEM. *Preprint SFB 393/99-32, TU Chemnitz*, 1999. to appear in Numer. Math.

[23] H. Harbrecht, F. Paiva, C. Pérez, and R. Schneider. Wavelet preconditioning for the coupling of FEM-BEM. *Preprint SFB 393/00-07, TU Chemnitz*, 2000. submitted to Numerical Linear Algebra with Applications.

[24] H. Harbrecht and R. Schneider. Wavelet Galerkin Schemes for 2D-BEM. In *Operator Theory: Advances and Applications*, volume 121. Birkhäuser, (2001).

[25] R. Kress. *Linear Integral Equations.* Springer-Verlag, Berlin-Heidelberg, 1989.

[26] T. von Petersdorff, R. Schneider, and C. Schwab. Multiwavelets for second kind integral equations. *SIAM J. Num. Anal.*, 34:2212–2227, 1997.

[27] T. von Petersdorff and C. Schwab. Fully discretized multiscale Galerkin BEM. In W. Dahmen, A. Kurdila, and P. Oswald, editors, *Multiscale wavelet methods for PDEs*, pages 287–346, Academic Press, San Diego, 1997.

[28] A. Rathsfeld. On a hierarchical three point basis of piecewise linear functions over smooth boundaries. In *Operator Theory: Advances and Applications*, volume 121. Birkhäuser, (2001).

[29] S. Sauter and C. Schwab. Quadrature for the *hp*-Galerkin BEM in $\mathbb{R}^3$. *Numer. Math.*, 78:211–258, 1997.

[30] R. Schneider. *Multiskalen- und Wavelet-Matrixkompression: Analysisbasierte Methoden zur Lösung großer vollbesetzter Gleichungssysteme.* B.G. Teubner, Stuttgart, 1998.

[31] W. Sweldens. The lifting scheme: A custom-design construction of biorthogonal wavelets. *Appl. Comput. Harmon. Anal.*, 3:186–200, 1996.

[32] E.E. Tyrtyshnikov. Mosaic sceleton approximation. *Calcolo*, 33:47–57, 1996.

[33] L. Villemoers. Wavelet analysis of refinement equations. *SIAM J. Math. Anal.*, 25:1433–1460, 1994.